Table 2
Association between *RASSF1A*, *CASP8*, *DCR2*, and *PCDHB* methylation and *MYCN* amplification.

	Group A1 (≤18 m)	Group A2 (≤18 m)	Group B (>18 m)		Group A2 (≤18 m)	Group B (>18 m)
RASSF1A (cMSP)				*RASSF1A* (qMSP)		
Total (methyl versus unmethyl)	NS	S (0.001)	S (0.002)		ROC, S (5.29E−06); DRR., S (8.97E−06)	ROC, S (0.003); DRR., S (0.001)
Diploidy (methyl versus unmethyl)	NS	S (0.005)	S (0.011)		ROC, S (0.002); DRR., S (0.001)	ROC, S (0.003); DRR., S (0.003)
Triploidy (methyl versus unmethyl)	NA	NA	NS		ROC, NA; DRR., NA.	ROC, M (0.08); DRR, NS
CASP8 (cMSP)						
Total (methyl versus unmethyl)	NS	S (1.94E−07)	S (0.002)			
Diploidy (methyl versus unmethyl)	NA	S (1.35E−04)	S (0.034)			
Triploidy (methyl versus unmethyl)	NA	NA	S (0.027)			
DCR2 (cMSP)				*DCR2* (qMSP)		
Total (methyl versus unmethyl)	NS	NS	NS		ROC, S (0.043); DRR., NA	ROC, NS; DRR., NS
Diploidy (methyl versus unmethyl)	NS	NS	NS		ROC, NS; DRR., NA.	ROC, NS; DRR., NS
Triploidy (methyl versus unmethyl)	NA	NA	NS		ROC, NA; DRR., NA.	ROC, NS; DRR., NS
PCDHB (cMSP)				*PCDHB (qMSP)*		
Total (methyl versus unmethyl)					ROC, S (2.34E−07); DRR., S (1.2E−04)	ROC, S (0.003); DRR., M (0.091)
Diploidy (methyl versus unmethyl)					ROC, S (5.86E−06); DRR., S (0.005)	ROC, S (0.036); DRR., S (0.032)
Triploidy (methyl versus unmethyl)					ROC, NA; DRR, NA.	ROC, NS; DRR., NS

Group A1, infants found by mass-screening; Group A2, infants diagnosed clinically; Group B, children diagnosed clinically; m, month; cMSP, conventional methylation-specific PCR; qMSP, quantitative methylation-specific PCR; Methyl, methylated; unmethyl, unmethylated; NS, not significant; S, significant; M, marginally significant; NA, not applicable; ROC, ROC analysis; DRR, dose–response relationship analysis; Detailed data are shown in Supplementary Tables 2–7.

children were at a more advanced stage than *DCR2*-unmethylated diploid and triploid tumors in children, respectively ($P = 0.003$ and $P = 0.017$), and the results were consistent with those obtained by quantitative MSP.

Quantitative MSP analysis disclosed that *PCDHB*-methylated diploid and triploid tumors were at more advanced stages than *PCDHB*-unmethylated diploid and triploid tumors, respectively, in children ($P = 0.001$ and $P = 0.003$). Such an association was not found between *PCDHB*-methylated and -unmethylated tumors in infants.

3.3. Correlation of methylation in the RASSF1A, CASP8, DCR2, and PCDHB genes with MYCN amplification

Because only 2 of 123 tumors found by mass-screening had *MYCN* amplification, further studies on the correlation were not conducted (Table 2). *RASSF1A* methylation detected by conventional MSP was associated with *MYCN* amplification in tumors in infants and children ($P = 0.001$ and $P = 0.002$). *CASP8* methylation was also associated with *MYCN* amplification in tumors in infants and children ($P = 1.94E{-}07$ and $P = 0.002$). In contrast, no association was found between *DCR2* methylation and *MYCN* amplification in tumors in infants and children. Quantitative MSP analysis in *RASSF1A* and *DCR2* methylation confirmed the findings. In addition, *PCDHB* methylation was also identified to have correlation with *MYCN* amplification in tumors of infants and children. The association between *RASSF1A* and *PCDHB* methylation and *MYCN* amplification was also indicated by different distributions of methylation percentages of *RASSF1A* and *PCDHB* between *MYCN*-amplified and –nonamplified tumors; however, different distributions of *DCR2* methylation percentages were not exhibited between the tumors in infants and children (Fig. 2).

We then classified tumors by the ploidy status, and found that none of the triploid tumors in infants had *MYCN* amplification. *RASSF1A* methylation was associated with *MYCN* amplification in diploid tumors in infants and children ($P = 0.005$ and $P = 0.011$), but not in triploid tumors in children. *DCR2* methylation was not associated with *MYCN* amplification in diploid and triploid tumors in children. Quantitative MSP analysis confirmed the association with *MYCN* amplification found in *RASSF1A*-methylated tumors, and no association found in *DCR2*-methylated tumors. *CASP8* methylation was associated with *MYCN* amplification in diploid tumors in infants ($P = 1.35E{-}04$) or in diploid and triploid tumors in children ($P = 0.034$ and $P = 0.027$). The correlation between *PCDHB* methylation and *MYCN* amplification was found in tumors of infants and children. When divided by the ploidy status, *RASSF1A* and *PCDHB* methylation was correlated with *MYCN* amplification in diploid, not triploid tumors in infants and children. *DCR2* methylation (>7%) was found only 3 of 53 tumors in infants; further study was not conducted. The correlation between *DCR2* methylation and *MYCN* amplification was not found in tumors of children.

3.4. Correlation between the methylation status of the RASSF1A, CASP8, DCR2, and PCDHB genes analyzed by conventional and quantitative MSP and overall survival

There was no prognostic significance of methylation of *RASSF1A*, *CASP8*, and *DCR2* in infants found by mass-screening because only two of 123 infants died of the disease (Table 3 and Supplementary Tables 2–4). When we combined infants and children clinically

Please cite this article in press as: M. Haruta et al., *RASSF1A* methylation may have two biological roles in neuroblastoma tumorigenesis depending on the ploidy status and age of patients, Cancer Lett. (2014), http://dx.doi.org/10.1016/j.canlet.2014.03.022

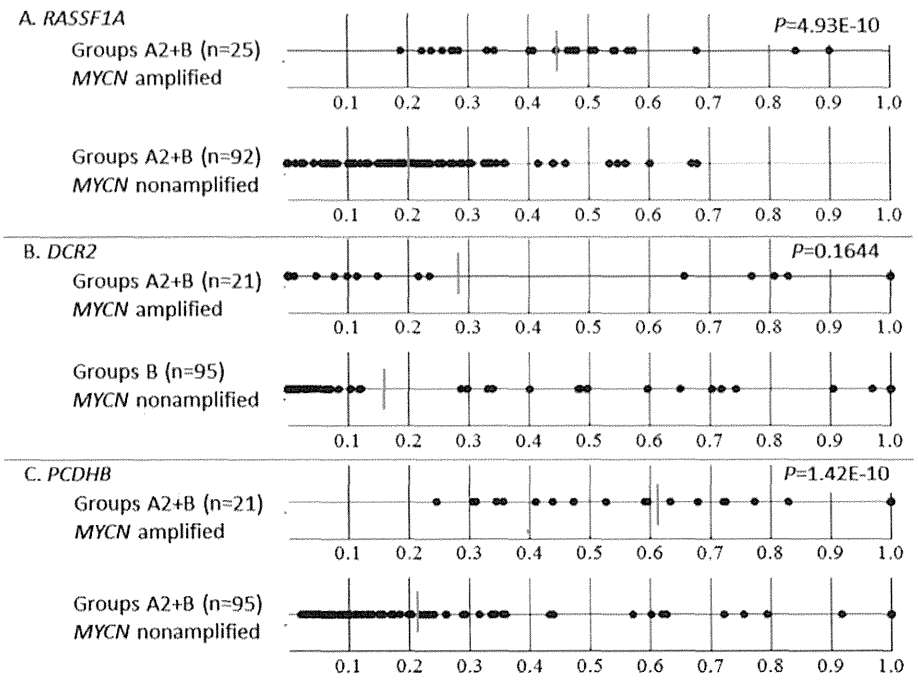

Fig. 2. The distribution of *RASSF1A*, *DCR2*, and *PCDHB* methylation percentages between *MYCN* amplified and *MYCN*-nonamplified tumors.

Table 3
Association between *RASSF1A*, *CASP8*, *DCR2*, and *PCDHB* methylation and overall survival.

	Group A1 (≤18 m)	Group A2 (≤18 m)	Group B (>18 m)		Group A2 (≤18 m)	Group B (>18 m)
RASSF1A (cMSP)				*RASSF1A* (qMSP)		
Total (methyl versus unmethyl)	NS	M (0.0705)	S (0.0331)		ROC, S (0.0001); DRR., S (0.0002)	ROC, S (0.0288); DRR., S (0.0060)
Diploidy (methyl versus unmethyl)	NS	S (0.0405)	NS		ROC, S (0.0057); DRR., S (0.0031)	ROC, NS; DRR., NS
Triploidy (methyl versus unmethyl)	NA	NS	NS		ROC, NA; DRR., NA	ROC, NS; DRR., S (0.0126)
CASP8 (cMSP)						
Total (methyl versus unmethyl)	NS	S (<0.0001)	NS			
Diploidy (methyl versus unmethyl)	NA	S (0.0027)	NS			
Triploidy (methyl versus unmethyl)	NA	NA	NS			
DCR2 (cMSP)				*DCR2* (qMSP)		
Total (methyl versus unmethyl)	NS	NA	M (0.0821)		ROC, S (0.0020); DRR., NA	ROC, NS; DRR., S (0.0360)
Diploidy (methyl versus unmethyl)	NA	NA	NS		ROC, S (0.0381); DRR., NA	ROC, NS; DRR., NS
Triploidy (methyl versus unmethyl)	NA	NA	S (0.0182)		ROC, NA; DRR., NA	ROC, NS; DRR., S (0.0164)
PCDHB (cMSP)				*PCDHB* (qMSP)		
Total (methyl versus unmethyl)					ROC, S (0.0101); DRR., S (<0.0001)	ROC, S (0.0218); DRR., NS
Diploidy (methyl versus unmethyl)					ROC, M (0.0609); DRR., S (0.0007)	ROC, NS; DRR., S (0.0451)
Triploidy (methyl versus unmethyl)					ROC, NA; DRR., NA	ROC, M (0.0850); DRR., NS

Group A1, infants found by mass-screening; Group A2, infants diagnosed clinically; Group B, children diagnosed clinically; m, month; cMSP, conventional methylation-specific PCR; qMSP, quantitative methylation-specific PCR; Methyl, methylated; unmethyl, unmethylated; NS, not significant; S, significant; M, marginally significant; NA, not applicable; ROC, ROC analysis; DRR, dose–response relationship analysis; Detailed data are shown in Supplementary Tables 2–7.

diagnosed, patients with a *RASSF1A*-, *CASP8*-, or *DCR2*-methylated tumor examined by conventional MSP had worse overall survival than patients with a *RASSF1A*-, *CASP8*-, or *DCR2*-unmethylated tumor, respectively ($P = 0.0015$, $P = 0.0003$, and $P = 0.0038$) (Fig. 3A–C).

When we further classified patients according to the ploidy status, infants with a *RASSF1A*-methylated diploid tumor had worse overall survival than infants with a *RASSF1A*-unmethylated diploid tumor ($P = 0.0405$); however, such an association was not found in infants with triploid tumors (Fig. 3D and F). In addition, infants with a *CASP8*-methylated diploid tumor had worse overall survival than infants with a *CASP8*-unmethylated diploid tumor ($P = 0.0027$). No significant difference was observed in overall

Please cite this article in press as: M. Haruta et al., *RASSF1A* methylation may have two biological roles in neuroblastoma tumorigenesis depending on the ploidy status and age of patients, Cancer Lett. (2014), http://dx.doi.org/10.1016/j.canlet.2014.03.022

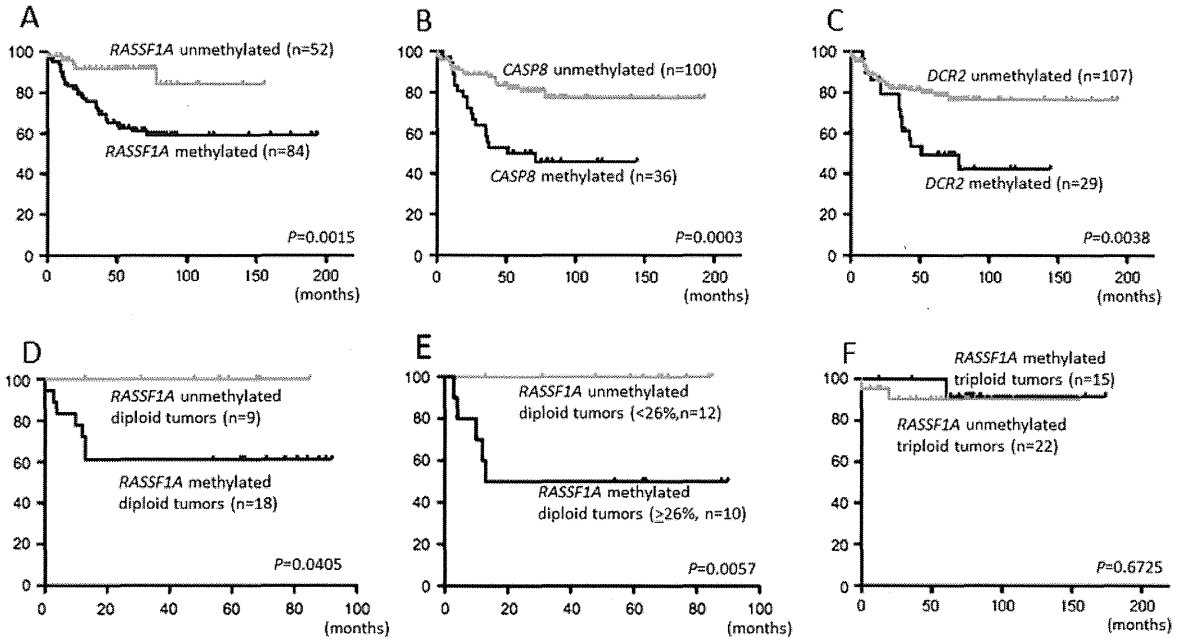

Fig. 3. Overall survival curves for infants and children diagnosed clinically and classified by the methylation status of *RASSF1A* (A), *CASP8* (B), and *DCR2* (C) examined by conventional MSP analysis. Overall survival curves for infants with a *RASSF1A*-methylated diploid tumor and those with a *RASSF1A*-unmethylated diploid tumor diagnosed clinically and examined by conventional MSP (D), or quantitative MSP (E) analysis, and for infants with a *RASSF1A*-methylated triploid tumor and those with a *RASSF1A*-unmethylated triploid tumor diagnosed clinically and examined by conventional MSP (F).

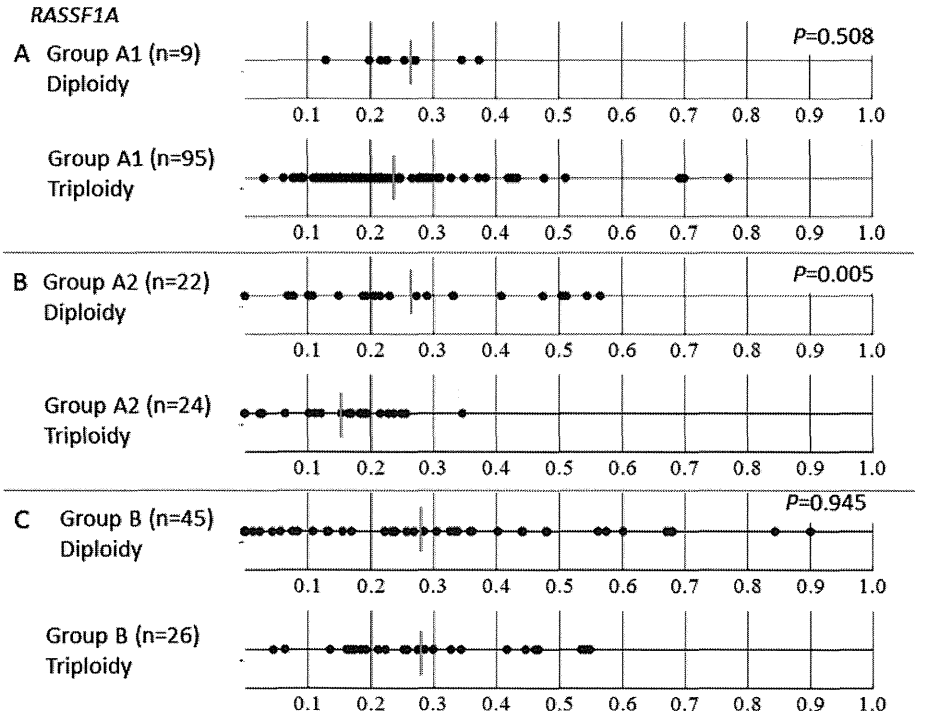

Fig. 4. The distribution of *RASSF1A* methylation percentages between diploid and triploid tumors in infants found by mass-screening (A), between diploid and triploid tumors in infants (<18 months) diagnosed clinically (B), and between diploid and triploid tumors in children (>18 months) (C).

survival between any two of the 4 types of tumors classified by the methylation status of *RASSF1A* or *CASP8* and the ploidy status in children. In contrast, children with a *DCR2*-methylated triploid tumor had worse overall survival than children with a *DCR2*-unmethylated triploid tumor ($P = 0.0182$).

When we analyzed *RASSF1A*, *DCR2*, and *PCDHB* methylation by quantitative MSP, an association between methylation of each gene and poor outcomes was identified in tumors of infants and children (Table 3). When we divided tumors according to the ploidy status, *RASSF1A* and *DCR2*, not *PCDHB* methylation was associated with a poor outcome in infants with a diploid, not triploid tumor. Interestingly, *RASSF1A* and *DCR2* methylation was correlated with a poor outcome in children with a triploid, not diploid tumor.

Please cite this article in press as: M. Haruta et al., *RASSF1A* methylation may have two biological roles in neuroblastoma tumorigenesis depending on the ploidy status and age of patients, Cancer Lett. (2014), http://dx.doi.org/10.1016/j.canlet.2014.03.022

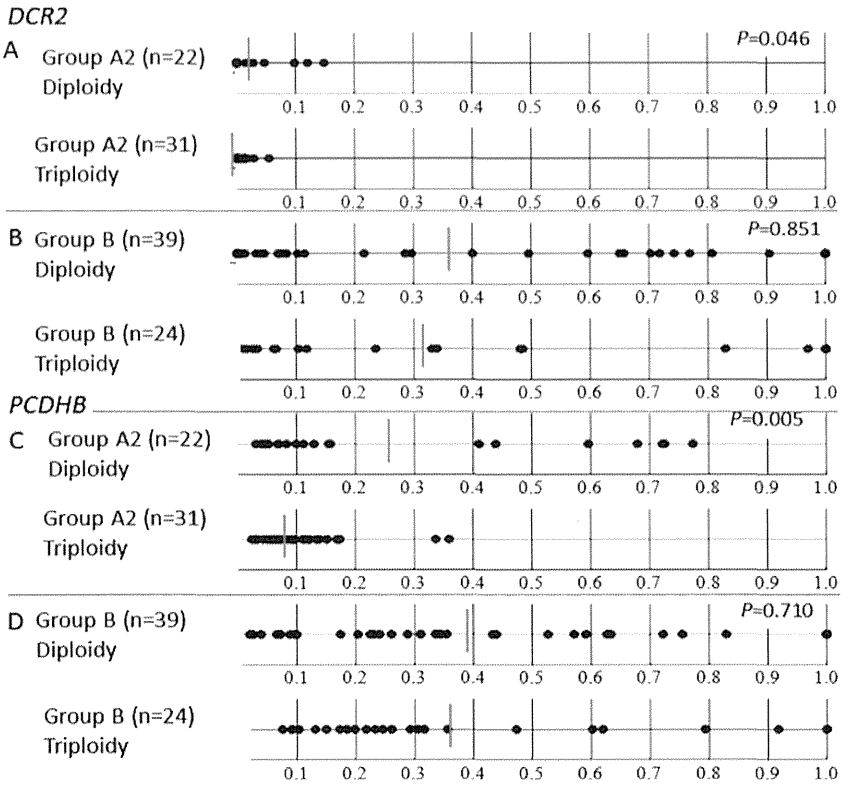

Fig. 5. The distribution of *DCR2* methylation percentages between diploid and triploid tumors in infants (<18 months) diagnosed clinically (A), and between diploid and triploid tumors in children (>18 months) (B). The distribution of *PCDHB* methylation percentages between diploid and triploid tumors in infants (<18 months) diagnosed clinically (C), and between diploid and triploid tumors in children (>18 months) (D).

Table 4
Multivariate analysis on 5 clinicopathological and genetic factors including *RASSF1A* methylation in 102 patients with neuroblastoma.

Prognostic factors	Relative risk (95%CI[a])	*P*-value	Relative risk (95%CI[a])	*P*-value
Age: ≤18 months versus > 18 months	2.07 (0.84–5.13)	0.1159	1.88 (0.75–4.70)	0.1754
Stage: 1, 2, 4S versus 3, 4	2.71 (0.79–9.27)	0.1116	2.88 (0.86–9.62)	0.0859
Ploidy: Triploidy versus diploidy	1.40 (0.65–3.01)	0.3940	1.26 (0.58–2.75)	0.5648
MYCN: Single copy versus amplification	3.19 (1.45–7.03)	0.0041	3.30 (1.55–7.00)	0.0019
RASSF1A [b]: Unmethylated (<26%) versus methylated (>26%)	1.55 (0.67–3.61)	0.3086		
RASSF1A [c]: Unmethylated (<40%) versus methylated (>40%)			2.19 (1.02–4.72)	0.0455

[a] 95%CI, 95% confidence interval.
[b] The cut-off value was determined by ROC analysis.
[c] The cut-off value was determined by the dose-response relationship.

3.5. The mean methylation percentage between diploid and triploid tumors in infants and children

The mean methylation percentage of *RASSF1A* was higher in diploid tumors than in triploid tumors of infants diagnosed clinically; however, such an association was not observed in tumors of infants found by mass-screening or children (Fig. 4). Likewise, the mean methylation percentage of *DCR2* or *PCDHB* was higher in diploid tumors than in triploid tumors of infants; however, such an association was not observed between diploid and triploid tumors in children (Fig. 5).

The difference in the methylation percentage of *RASSF1A* or *DCR2* between diploid and triploid tumors in infants, but not in children reflected the difference in outcomes between infants having a diploid tumor with or without *RASSF1A* or *DCR2* methylation ($P = 0.0057$ and $P \approx 0.0381$), but not between children having a diploid tumor with or without (Table 3). Interestingly, the difference in outcomes was observed between children having a triploid tumor with or without *RASSF1A* or *DCR2* methylation, but not between infants having a triploid tumor with or without; methylation percentages of *RASSF1A* or *DCR2* rarely exceeded cut-off values of 27% or 7% in triploid tumors in infants (Figs. 4 and 5).

3.6. Multivariate Cox proportional hazard regression analysis on 5 clinical and genetic factors in 102 patients clinically diagnosed

Multivariate analysis exhibited the *MYCN* amplification and *RASSF1A* methylation statuses were shown to be independent factors predicting poor outcome, but the *PCDHB* and *DCR2* methylation statuses were not (Table 4, and Supplementary Tables 8 and 9).

4. Discussion

The present study using conventional MSP found methylation of the *RASSF1A*, *CASP8*, and *DCR2* genes in 62%, 25%, and 21%, respectively, of 136 neuroblastoma samples diagnosed clinically. Previous studies reported methylation of *RASSF1A*, *CASP8*, and *DCR2* in

Please cite this article in press as: M. Haruta et al., *RASSF1A* methylation may have two biological roles in neuroblastoma tumorigenesis depending on the ploidy status and age of patients, Cancer Lett. (2014), http://dx.doi.org/10.1016/j.canlet.2014.03.022

Table 5
Incidences and associations between *RASSF1A*, *CASP8*, and *DCR2* methylation and disease stage, *MYCN* amplification, and overall or event-free survival.

Studies	*RASSF1A*				*CASP8*				*DCR2*			
	Incidence	Stage	*MYCN* amp.	Survival	Incidence	Stage	*MYCN* amp.	Survival	Incidence	Stage	*MYCN* amp.	Survival
Astuti et al. [14]	55%, 37/67	N. S.	N. S.	N. S.	40%, 24/60	N. D.	N. D.	N. D.				
Yang et al. [15]	70%, 39/56	N. S.	N. S.	OS, $P < 0.01$								
Banelli et al. [16]	84%, 26/31	N. D.	$P < 0.05$	OS, N. S.		N. D.	N. S.	N. D.	42%, 13/31	N. D.	N. S.	OS, $P < 0.03$
Lázcoz et al. [17]	83%, 29/35	N. D.	N. S.	N. D.	60%, 21/35	N. D.	N. S.	N. D.				
Yang et al. [18]	90%, 63/70	N. D.	N. D.	N. D.	56%, 39/70	N. D.	N. S.	OS, $P = 0.008$	44%, 31/70	N. D.	N. D.	OS, $P = 0.019$
Michalowski et al. [19]	93%, 42/45	N. D.	N. D.	N. S.	38%, 17/45	$P = 0.001$	N. S.	N. S.				
Misawa et al. [20]	94%, 64/68	N. S.	N. S.	N. S.								
Hoebeeck et al. [21]	71%, 29/41	N. S.	N. S.	OS and EFS, N. S.	56%, 20/36	N. S.	N. S.	EFS, $P = 0.038$				
Grau et al. [22]	66%, 54/82	$P = 0.024$	N. S.	EFS, $P = 0.003$ (intermediate risk)	52%, 43/8	$P < 0.001$	$P = 0.007$	OS, $P = 0.019$ EFS, $P = 0.002$				
Stutterheim et al. [23]	96%, 68/71	N. D.	St 1–3, $P = 0.006$ St 4, $P = 0.05$	OS, $P = 0.02$ (St 4 & > 1 y.)								
Kiss et al. [24]	61%, 23/38	N. D.	N. D.	N. D.	55%, 21/38	N. D.	N. S.	N. D.				
Teitz et al. [25]					62%, 26/42	N. S.	$P < 0.0001$	N. D.				
Takita et al. [26]					32%, 8/25	N. D.	N. S.	N. D.				
Gonzalez-Gomez et al. [27]					14%, 6/38	$P = 0.019$	$P = 0.0047$	N. D.				
Asada et al. [28]					19%, 26/140 20%, 30/152	N. D.	N. D.	OS $P = 0.002$ in Japanese $P = 0.0002$ in German				
van Noesel et al. [29]									70%, 39/56	N. D.	N. D.	N. D.
Yagyu et al. [30]									28%, 24/86	N. D.	N. D.	OS, $P = 0.008$ EFS, $P < 0.001$
Present study	62%, 84/136	<18 m, $P = 0.018$ >18 m, $P < 0.001$	$P < 0.001$	OS, $P = 0.0015$	27%, 36/136	<18 m $P = 0.090$ >18 m $P = 0.026$	$P = 0.0003$	OS, $P < 0.001$	21%, 29/136	<18 m, $P = 0.406$ >18 m, $P < 0.001$	$P = 0.149$	OS, $P = 0.0038$

N. S., not significant; N. D., not done; OS, overall survival; EFS, event-free survival; st, stage; 1 y., one year; Studies were cited in the Reference section.

55–96%, 14–62%, and 28–70% in 25–86 neuroblastoma samples (Table 5) [14–30]. The various results may have been affected by the location of primers for target genes and numbers of PCR cycles used for conventional and quantitative MSP analysis. We also evaluated *PCDHB* methylation, which was reported in a substantial number of neuroblastoma samples [31].

Regarding to methylation of the 4 genes and the stage distribution, *RASSF1A* methylation was associated with a more advanced stage in infants and children diagnosed clinically and in infants with a diploid tumor found by mass-screening, whereas *CASP8*, *DCR2*, and *PCDHB* methylation was associated with an advanced stage only in tumors of children (Table 1). The findings reflected that *RASSF1A* methylation was fairly common in neuroblastoma in infants, while *CSAP8*, *DCR2*, and *PCDHB* methylation was rare in tumors of infants, especially in triploid tumors.

Associations between *RASSF1A*, or *CASP8* methylation and *MYCN* amplification have been reported (Table 5) [14–28]. In addition, neuroblastoma with *PCDHB* methylation was reported to include all tumors with *MYCN* amplification, and associated with a poor outcome [31]. The present study exhibited that *RASSF1A*, *CASP8*, or *PCDHB* methylation was correlated with *MYCN* amplification in tumors of infants and children, but *DCR2* methylation was not (Table 2 and Fig. 2). Based on classification by the ploidy status, the association between *RASSF1A* or *PCDHB* methylation and *MYCN* amplification was observed in diploid tumors of infants and children; triploid tumors in infants had no *MYCN* amplification, therefore, associations could not be examined. *CASP8* methylation was associated with *MYCN* amplification in diploid tumors of infants and children, and triploid tumors in children.

Regarding to overall survival, the present study using conventional and/or quantitative MSP analysis exhibited association between *RASSF1A*, *DCR2*, and *PCDHB* methylation and poor outcomes in infants and children (Table 3 and Fig. 1), especially in diploid tumors of infants, and triploid tumors of children; *CASP8* methylation was only associated with a poor outcome in infants with a diploid tumor. Thus, *RASSF1A* methylation was associated with at a more advanced stage, *MYCN* amplification, and a poor outcome in infants with a diploid tumor. Although a substantial number of triploid tumors in infants exhibited *RASSF1A* methylation by conventional MSP analysis, they had no *MYCN* amplification and showed a favorable outcome, suggesting triploid tumors in infants as a specific biological subtype of neuroblastoma. Children with *RASSF1A*-, *DCR2*-, and *PCDHB*-methylated tumors had poorer outcomes than children with *RASSF1A*-, *DCR2*-, and *PCDHB*-unmethylated tumors, respectively. The association between *RASSF1A* and *DCR2* methylation and a poor outcome in children with triploid tumors is noteworthy, because the association was also observed in infants having a diploid tumor with or without *RASSF1A* and *DCR2* methylation. These findings suggest 2 subtypes of triploid neuroblastoma; while one was common in infants, exhibited hypomethylation of *RASSF1A* and *DCR2*, no *MYCN* amplification, and a favorable outcome, the other was common in children, exhibited hypermethylation of *RASSF1A*, *DCR2*, and *PCDHB*, frequent *MYCN* amplification, and an unfavorable outcome. We previously stated that triploidy in infant neuroblastoma may arisen through tetraploidization and succeeding tripolar division, whereas triploidy in childhood neuroblastoma may have derived from tetraploidization and chromosome loss [36]. We suggest that different mechanisms of triploid formation may have contributed to the different epigenetic features between infant and childhood triploid tumors. INRG proposed that patients with a hyperdiploid tumor be classified at low risk, whereas patients with a diploid tumor be classified at intermediate risk if they were $\leqslant$18 months of age and at the distantly metastatic stage [33]. We provided the data on epigenetic differences between diploid and triploid tumors in infants, and supported the inclusion of the ploidy status as one of factors included in the INRG classification system.

A recent study proposed a model in which the binding of TNFα to the death receptor, TNFαR1 results in its internalization, and subsequent formation of a complex with MOAP-1/RASSF1A to promote the open form of MOAP-1 to associate with Bax. This in turn results in Bax conformational changes and recruitment to the mitochondria to initiate cell death [10]. Silencing of *RASSF1A* due to promoter methylation by DNMT3B facilitated by MYCN and PRC2 was shown to avoid neuroblastoma cells entering apoptosis [37]. Thus, we consider that *RASSF1A*-methylated diploid tumors avoid entering apoptosis, facilitate proliferation, and finally cause unfavorable outcomes in infants and children with overexpressed MYCN with or without *MYCN* amplification.

On the other hand, aneuploidy has been shown to cause a proliferative disadvantage in yeast because of the overexpression of certain metabolism-associated genes [38], and it has been speculated that hypermethylation of the promoter regions of genes in cancer cells may lessen the metabolic impact of aneuploidy by silencing genes on a supernumerary chromosome while preserving the expression of other genes on chromosome that confer a selective advantage [39]. We propose that *RASSF1A* methylation in triploid neuroblastomas in infants found by mass-screening or diagnosed clinically may modulate their expression levels to repress cell cycle arrest and microtubule stabilization.

DCR2 is an antiapoptotic decoy receptor, which disturbs TRAIL-induced apoptosis in normal cells [29]. The present findings showing that *MYCN* amplification was associated with *RASSF1A*, *CASP8*, and *PCDHB* methylation, but not with *DCR2* methylation, may be explained by the transcriptional regulation of MYCN to the *RASSF1A*, *CASP8*, and *PCDHB* promoters, but not to the *DCR2* promoter.

In conclusion, the present study disclosed 2 subtypes of triploid neurblastoma with different clinical and epigenetic characteristics. These findings will facilitate understanding of heterogeneous biology of neuroblastoma, and improve choice of the treatment.

Conflict of interest

None.

Appendix A. Supplementary material

Supplementary data associated with this article can be found, in the online version, at http://dx.doi.org/10.1016/j.canlet.2014.03.022.

References

[1] J.M. Maris, M.D. Hogarty, R. Bagatell, S.L. Cohn, Neuroblastoma, Lancet 369 (2007) 2106–2115.
[2] G.M. Brodeur, Neuroblastoma: biological insights into a clinical enigma, Nat. Rev. Cancer 3 (2003) 203–216.
[3] M. Schwab, F. Westermann, B. Hero, F. Berthold, Neuroblastoma: biology and molecular and chromosomal pathology, Lancet Oncol. 4 (2003) 472–480.
[4] T. Sawada, M. Hirayama, T. Nakata, T. Takeda, N. Takasugi, T. Mori, et al., Mass screening for neuroblastoma in infants in Japan, Lancet 2 (1984) 271–273.
[5] W.G. Wood, R.N. Gao, J.J. Shuster, L.L. Robison, M. Bernstin, S. Weitzman, et al., Screening of infants and mortality due to neuroblastoma, N. Engl. J. Med. 346 (2002) 1041–1046.
[6] F.H. Schilling, C. Spix, F. Berthold, R. Erttmann, N. Fehse, B. Hero, et al., Neuroblastoma screening at one year of age, N. Engl. J. Med. 346 (2002) 1047–1053.
[7] E. Hiyama, T. Iehara, T. Sugimoto, M. Fukuzawa, Y. Hayashi, F. Sasaki, et al., Effectiveness of screening for neuroblastoma at 6 months of age: a retrospective population-based cohort study, Lancet 371 (2008) 1173–1180.
[8] A. Agathanggelou, W.N. Cooper, F. Latif, Role of the Ras-association domain family 1 tumor suppressor gene in human cancer, Cancer Res. 65 (2005) 3497–3508.
[9] A.M. Richter, G.P. Pfeifer, R.H. Dammann, The RASSF proteins in cancer; from epigenetic silencing to functional characterization, Biochim. Biophys. Acta 1796 (2009) 114–128.

[10] M. Gordon, S. Baksh, RASSF1A: not a prototypical Ras effector, Small GTPases 2 (2011) 148–157.
[11] S. Honda, M. Haruta, W. Sugawara, F. Sasaki, M. Ohira, T. Matsunaga, et al., The methylation status of *RASSF1A* promoter predicts responsiveness to chemotherapy and eventual cure in hepatoblastoma patients, Int. J. Cancer 123 (2008) 1117–1125.
[12] J. Wang, B. Wang, X. Chen, J. Bi, The prognostic value of RASSF1A promoter hypermethylation in non-small cell lung carcinoma: a systematic review and meta-analysis, Carcinogenesis 32 (2011) 441–446.J.
[13] J. Ohshima, M. Haruta, Y. Fujiwara, N. Watanabe, Y. Arai, T. Ariga, et al., Methylation of the *RASSF1A* promoter is predictive of poor outcome among patients with Wilms tumor, Ped. Blood Cancer 59 (2012) 499–505.
[14] D. Astuti, A. Agathanggelou, S. Honorio, A. Dallol, T. Martinsson, P. Kogner, et al., *RASSF1A* promoter region CpG island hypermethylation in phaeochromocytomas and neuroblastoma tumours, Oncogene 20 (2001) 7573–7577.
[15] Q. Yang, P. Zage, D. Kagan, Y. Tian, R. Seshadri, H.R. Salwen, et al., Association of epigenetic inactivation of *RASSF1A* with poor outcome in human neuroblastoma, Clin. Cancer Res. 10 (2004) 8493–8500.
[16] B. Banelli, I. Gelvi, A. Di Vinci, P. Scaruffi, I. Casciano, G. Allemanni, et al., Distinct CpG methylation profiles characterize different clinical groups of neuroblastic tumors, Oncogene 24 (2005) 5619–5628.
[17] P. Lázcoz, J. Muñoz, M. Nistal, A. Pestaña, I. Encío, J.S. Castresana, Frequent promoter hypermethylation of RASSF1A and CASP8 in neuroblastoma, BMC Cancer 6 (2006) 254–264.
[18] Q. Yang, C.M. Kiernan, Y. Tian, H.R. Salwen, A. Chlenski, B.A. Brumback, et al., Methylation of *CASP8*, *DCR2*, and *HIN-1* in neuroblastoma is associated with poor outcome, Clin. Cancer Res. 13 (2007) 3191–3197.
[19] M.B. Michalowski, F. Fraipont, D. Plantaz, S. Michelland, V. Combaret, M.C. Favrot, Methylation of tumor-suppressor genes in neuroblastoma: the RASSF1A gene is almost always methylated in primary tumors, Ped. Blood Cancer 50 (2008) 29–32.
[20] A. Misawa, S. Tanaka, S. Yagyu, K. Tsuchiya, T. Iehara, T. Sugimoto, et al., *RASSF1A* hypermethylation in pretreatment serum DNA of neuroblastoma patients: a prognostic marker, Br. J. Cancer 100 (2009) 399–404.
[21] J. Hoebeeck, E. Michels, F. Pattyn, V. Combaret, J. Vermeulen, N. Yigit, et al., Aberrant methylation of candidate tumor suppressor genes in neuroblastoma, Cancer Lett. 273 (2009) 336–346.
[22] E. Grau, F. Martinez, C. Orellana, A. Canete, Y. Yañez, S. Oltra, et al., Hypermethylation of apoptotic genes as independent prognostic factor in neuroblastoma disease, Mol Carcinog. 50 (2011) 153–162.
[23] J. Stutterheim, F.A. Ichou, E. Ouden, R. Versteeg, H.N. Caron, G.A. Tytgat, et al., Methylated RASSF1a is the first specific DNA marker for minimal residual disease testing in neuroblastoma, Clin. Cancer Res. 18 (2012) 808–814.
[24] N.B. Kiss, P. Kogner, J.I. Johnsen, T. Martinsson, C. Larsson, J. Geli, Quantitative global and gene-specific promoter methylation in relation to biological properties of neuroblastomas, BMC Med. Genet. (2012), http://dx.doi.org/10.1186/1471-2350-13-83.
[25] T. Teitz, T. Wei, M.B. Valentine, E.F. Vanin, J. Grenet, V.A. Valentine, et al., Caspase 8 is deleted or silenced preferentially in childhood neuroblastomas with amplification of *MYCN*, Nat. Med. 6 (2000) 529–535.
[26] J. Takita, H.W. Yang, Y.Y. Chen, R. Hanada, K. Yamamoto, T. Teitz, et al., Allelic imbalance on chromosome 2q and alterations of the caspase 8 gene in neuroblastoma, Oncogene 20 (2001) 4424–4432.
[27] P. Gonzalez-Gomez, M.J. Bello, J. Lomas, D. Arjona, M.E. Alonso, C. Amiñoso, et al., Aberrant methylation of multiple genes in neuroblastic tumours: relationship with *MYCN* amplification and allelic status at 1p, Eur. J. Cancer 39 (2003) 1478–1485.
[28] K. Asada, N. Watanabe, Y. Nakamura, M. Ohira, F. Westermann, M. Schwab, A. Nakagawara, T. Ushijima, Stronger prognostic power of the CpG island methylator phenotype than methylation of individual genes in neuroblastomas, Jpn. J. Clin. Oncol. 43 (2013) 641–645.
[29] M.M. van Noesel, S. Bezouw, G.S. Salomons, P.A. Voûte, R. Pieters, S.B. Baylin, et al., Tumor-specific down-regulation of the tumor necrosis factor-related apoptosis-inducing ligand decoy receptors DcR1 and DcR2 is associated with dense promoter hypermethylation, Cancer Res. 62 (2002) 2157–2161.
[30] S. Yagyu, T. Gotoh, T. Iehara, M. Miyachi, Y. Katsumi, S. Tsubai-Shimizu, et al., Circulating methylated-*DCR2* gene in serum as an indicator of prognosis and therapeutic efficacy in patients with *MYCN* nonamplified neuroblastoma, Clin. Cancer Res. 14 (2008) 7011–7019.
[31] M. Abe, M. Ohira, A. Kaneda, Y. Yagi, S. Yamamoto, Y. Kitano, T. Takato, A. Nakagawara, T. Ushijima, CpG island methylator phenotype is a strong determinant of poor prognosis in neuroblastomas, Cancer Res. 65 (2005) 828–834.
[32] Y. Kaneko, H. Kobayashi, N. Watanabe, N. Tomioka, A. Nakagawara, Biology of neuroblastomas that were found by mass screening at 6 months of age in Japan, Ped. Blood Cancer 46 (2006) 285–291.
[33] S.L. Cohn, A.D. Pearson, W.B. London, T. Monclair, P.F. Ambros, G.M. Brodeur, et al., The International Neuroblastoma Risk Group (INRG) classification system: an INRG task force report, J. Clin. Oncol. 27 (2009) 289–297.
[34] Y. Kaneko, H. Kobayashi, N. Maseki, A. Nakagawara, M. Sakurai, Disomy 1 with terminal 1p deletion was frequent in mass screening-negative/late-presenting neuroblastomas in young children, but not in mass screening-positive neuroblastomas in infants, Int. J. Cancer 80 (1999) 54–59.
[35] J.G. Herman, J.R. Graff, S. Myöhänen, B.D. Nelkin, S.B. Baylin, Methylation-specific PCR: a novel PCR assay for methylation status of CpG islands, Proc. Natl. Acad. Sci. USA 93 (1996) 9821–9826.
[36] Y. Kaneko, A.G. Knudson, Mechanism and relevance of ploidy in neuroblastoma, Genes Chromosomes Cancer 29 (2000) 89–95.
[37] R.K. Palakurthy, N. Wajapeyee, M.K. Santra, C. Gazin, L. Lin, S. Gobeil, et al., Epigenetic silencing of the *RASSF1A* tumor suppressor gene through HOXB3-mediated induction of *DNMT3B* expression, Mol. Cell 36 (2009) 219–230.
[38] T. Galitski, A.J. Saldanha, C.A. Styles, E.S. Lander, G.R. Fink, Ploidy regulation of gene expression, Science 285 (1999) 251–254.
[39] P.V. Jallepalli, D. Pellman, Cell biology. Aneuploidy in the balance, Science 317 (2007) 904–905.

Please cite this article in press as: M. Haruta et al., *RASSF1A* methylation may have two biological roles in neuroblastoma tumorigenesis depending on the ploidy status and age of patients, Cancer Lett. (2014), http://dx.doi.org/10.1016/j.canlet.2014.03.022

Oncogene (2014), 1–12

www.nature.com/onc

ORIGINAL ARTICLE

Receptor-type protein tyrosine phosphatase κ directly dephosphorylates CD133 and regulates downstream AKT activation

O Shimozato[1], M Waraya[1], K Nakashima[1], H Souda[2], N Takiguchi[2], H Yamamoto[2], H Takenobu[1], H Uehara[1], E Ikeda[1], S Matsushita[3], N Kubo[3], A Nakagawara[4], T Ozaki[3] and T Kamijo[1,5]

Although CD133 has been considered to be a molecular marker for cancer stem cells, its functional roles in tumorigenesis remain unclear. We here examined the molecular basis behind CD133-mediated signaling. Knockdown of CD133 resulted in the retardation of xenograft tumor growth of colon cancer-derived HT-29 and LoVo cells accompanied by hypophosphorylation of AKT, which diminished β-catenin/T-cell factor-mediated CD44 expression. As tyrosine residues of CD133 at positions 828 and 852 were phosphorylated in HT-29 and SW480 cells, we further addressed the significance of this phosphorylation in the tumorigenesis of SW480 cells expressing mutant CD133, with substitution of these tyrosine residues by glutamate (CD133-EE) or phenylalanine (CD133-FF). Forced expression of CD133-EE promoted much more aggressive xenograft tumor growth relative to wild-type CD133-expressing cells accompanied by hyperphosphorylation of AKT; however, CD133-FF expression had negligible effects on AKT phosphorylation and xenograft tumor formation. Intriguingly, the tyrosine phosphorylation status of CD133 was closely linked to the growth of SW480-derived spheroids. Using yeast two-hybrid screening, we finally identified receptor-type protein tyrosine phosphatase κ (PTPRK) as a binding partner of CD133. *In vitro* studies demonstrated that PTPRK associates with the carboxyl-terminal region of CD133 through its intracellular phosphatase domains and also catalyzes dephosphorylation of CD133 at tyrosine-828/tyrosine-852. Silencing of PTPRK elevated the tyrosine phosphorylation of CD133, whereas forced expression of PTPRK reduced its phosphorylation level markedly and abrogated CD133-mediated AKT phosphorylation. Endogenous CD133 expression was also closely associated with higher AKT phosphorylation in primary colon cancer cells, and ectopic expression of CD133 enhanced AKT phosphorylation. Furthermore, lower PTPRK expression significantly correlated with the poor prognosis of colon cancer patients with high expression of CD133. Thus, our present findings strongly indicate that the tyrosine phosphorylation of CD133, which is dephosphorylated by PTPRK, regulates AKT signaling and has a critical role in colon cancer progression.

Oncogene advance online publication, 2 June 2014; doi:10.1038/onc.2014.141

INTRODUCTION

Colon cancer is the third leading cause of death from cancer and is responsible for over 50 000 deaths in the United States.[1] Although substantial progress has been made in the past decade, relapse and metastasis to other tissues are serious issues to be addressed to cure colorectal cancer.[2] In this regard, understanding the molecular mechanism(s) underlying colon cancer aggressiveness is essential to improve the treatment of colon malignancy. In several malignancies, including colon cancer, breast cancer and brain tumor, a small population of tumor cells, the so-called cancer stem cells (CSCs),[3] has been shown to possess the capacity to initiate tumor growth. Some CSCs are resistant to extensive chemotherapy owing to the overexpression of multidrug-resistant *ABCG2*.[4] Thus, CSC has been considered to be a cause of relapse and a promising cellular target in the development of a novel therapeutic strategy for cancers.[5]

CD133, also known as Prominin-1, is a unique five-transmembrane glycoprotein initially identified in CD34-positive hematopoietic stem cells.[6,7] In addition, CD133 was expressed in stem/progenitor cells of various tissues, including the kidney, neuron and pancreas.[8–11] In the murine intestine, CD133-positive ($CD133^+$) cells were localized at the bottom of the intestinal crypt and had the potential to differentiate into mature intestinal epithelial cells.[12] Intriguingly, several lines of evidence indicate that CD133 acts as a potential CSC marker for several malignancies. In support of this notion, it has been shown that $CD133^+$ cells display tumorigenic activity in immunodeficient animals, self-renewal capacity and a chemoresistant phenotype.[13–19] Recent studies have revealed that the CD133 expression level is a marker of the prognostic impact of colon cancer.[20–22] Further studies have demonstrated that activation of WNT/β-catenin, Notch signaling and AKT-Bad-Bcl-2 pathways affect the behavior of $CD133^+$ cells.[23–25] Thus, it is likely that elucidation of the molecular mechanism(s) underlying high tumorigenic activity of $CD133^+$ tumors will contribute to the development of CSC-targeted therapy.

Tyrosine phosphorylation of CD133 has been shown in human brain tumor cell lines using an *in vitro* kinase reaction;[26] however,

[1]Division of Biochemistry and Molecular Carcinogenesis, Chiba Cancer Center Research Institute, Chiba, Japan; [2]Department of Gastrointestinal Surgery, Chiba Cancer Center Hospital, Chiba, Japan; [3]Laboratory of DNA Damage Signaling, Chiba Cancer Center Research Institute, Chiba, Japan; [4]Division of Biochemistry and Innovative Cancer Therapeutics, Chiba Cancer Center Research Institute, Chiba, Japan and [5]Research Institute for Clinical Oncology, Saitama Cancer Center, Saitama, Japan. Correspondence: Professor T Kamijo, Research Institute for Clinical Oncology, Saitama Cancer Center, 818 Komuro, Ina, Saitama 362-0806, Japan.
E-mail: tkamijo@cancer-c.pref.saitama.jp
Received 2 December 2013; revised 2 April 2014; accepted 10 April 2014

its functional significance in the regulation of tumor initiation and/or progression remains elusive. Our previous study demonstrated that CD133 is closely linked to phosphatidylinositol 3-kinase (PI3K)/AKT activation.[27] This observation prompted us to examine the possible role of the tyrosine phosphorylation of CD133 in the regulation of AKT activation during colon carcinogenesis. In the present study, we found for the first time that tyrosine phosphorylation of CD133 regulates colon cancer progression via AKT/β-catenin activation. Furthermore, we here identified the receptor-type protein tyrosine phosphatase κ (PTPRK) as a novel binding partner of CD133, which has the ability to dephosphorylate CD133.

RESULTS

Knockdown of CD133 suppresses xenograft tumor formation and anchorage-independent proliferation of human colorectal cancer cells

To examine the possible role(s) of CD133 in tumorigenesis, we transduced a short hairpin RNA-bearing lentivirus into $CD133^+$ human colon cancer-derived HT-29 and LoVo cells. Marked reduction of CD133 at mRNA and protein levels was observed in these cells (Figure 1a). CD133-knockdown (CD133-KD) cells, their mock-transduced cells or their parental cells were then subcutaneously inoculated into nude mice, and the tumors were measured at the indicated times after inoculation. CD133-KD tumors were significantly smaller than their parental and mock-transduced tumors 21 and 24 days after inoculation (Figure 1b; $P=0.005$, analysis of variance (ANOVA)). To confirm these results *in vitro*, we examined the anchorage-independent proliferation of CD133-KD cells. Stable knockdown of CD133 led to a significant decrease in the number of colonies arising from HT-29 and LoVo cells in soft agar medium (Figure 1c). In contrast, silencing of CD133 did not affect the cellular proliferation of either cell line *in vitro* (Supplementary Figure S1).

CD133 activates the AKT/β-catenin pathway and induces its target CD44 expression

Our previous studies showed that a PI3K inhibitor impairs CD133-mediated neuroblastoma differentiation,[27] suggesting the existence of a functional collaboration between PI3K and CD133. We examined whether PI3K could be attenuated in CD133-KD cells. To this end, CD133-KD HT-29 cells were treated with or without a PI3K inhibitor LY294002 and then their viability was

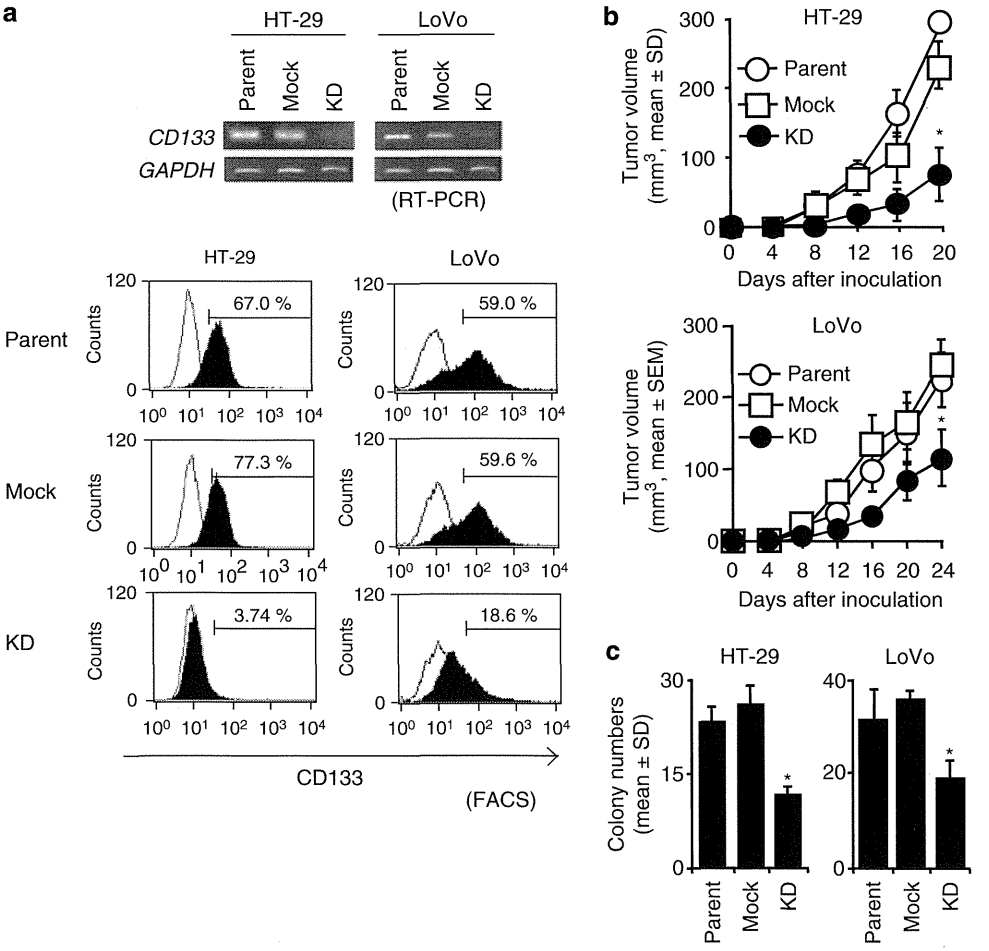

Figure 1. Knockdown of CD133 suppresses xenograft tumor formation and anchorage-independent proliferation of human colorectal cancer cells. (**a**) Generation of CD133-KD cells. CD133 was knocked down with HT-29 and LoVo cells as described in the Materials and methods section. CD133 expression was evaluated by semiquantitative RT–PCR and flow cytometry. (**b**) Xenograft tumor growth. Cells ($1x10^6$ cells) were subcutaneously inoculated into the flanks of BALB/c nude mice ($n=3$). Tumor volumes of parental (open circles), mock-transduced (open squares) and CD133-KD (closed circles) cells at the indicated times. Asterisks indicate statistical differences between CD133-KD and either parental or mock-transduced (Mock) cells ($P<0.05$, ANOVA). (**c**) Anchorage-independent cell growth. Parent, Mock and CD133-KD cells were cultured in the soft agar medium for 2 weeks and then the number of colonies was counted ($n=3$). Asterisks indicate statistical difference between CD133-KD and either parental or Mock cells ($P<0.05$, ANOVA).

measured because blockade of PI3K might promote cell death in several tumor cells.[28–30] CD133-KD cells exhibited higher sensitivity to LY294002-induced cell death than mock-transduced cells (Figure 2a). As AKT is one of the major effectors in a pathway triggered by PI3K, we evaluated the phosphorylation level of AKT in CD133-KD cells. As expected, the phosphorylation level of AKT at serine-473[31] and threonine-308[32] was significantly reduced in CD133-KD HT-29 and LoVo cells relative to that of mock-transduced cells. In contrast, the expression level of phosphatase and tensin homolog (PTEN), which acts as a negative regulator of the PI3K pathway,[33] remained unchanged regardless of CD133 expression (Figure 2b).

Our present results raised the possibility that CD133 might be closely involved in the regulation of the AKT/β-catenin signaling pathway. We therefore investigated the phosphorylation status of β-catenin in CD133-KD cells, which has been shown to be one of the substrates of AKT.[34] Silencing of CD133 reduced the steady-state phosphorylation level of β-catenin at serine-552 (Figure 2c) and also led to a decrease in the amount of nuclear β-catenin (Figure 2d). Under our experimental conditions, lamin B was used as a nuclear marker and E-cadherin was not detectable in the nuclear fraction (data not shown).

We next examined the possible effect of CD133 on the transactivation ability of β-catenin/T-cell factor (TCF) complex using a luciferase reporter driven by a β-catenin/TCF complex-responsive element. Luciferase activity was significantly lower in CD133-KD HT-29 cells than in mock-transduced cells (Figure 2e; $P=0.011$, *t*-test). Consistent with these results, silencing of CD133 also resulted in marked downregulation of CD44 at mRNA and protein levels, which has been shown to be a β-catenin/TCF complex target gene (Figure 2f and Supplementary Figure S2).[35]

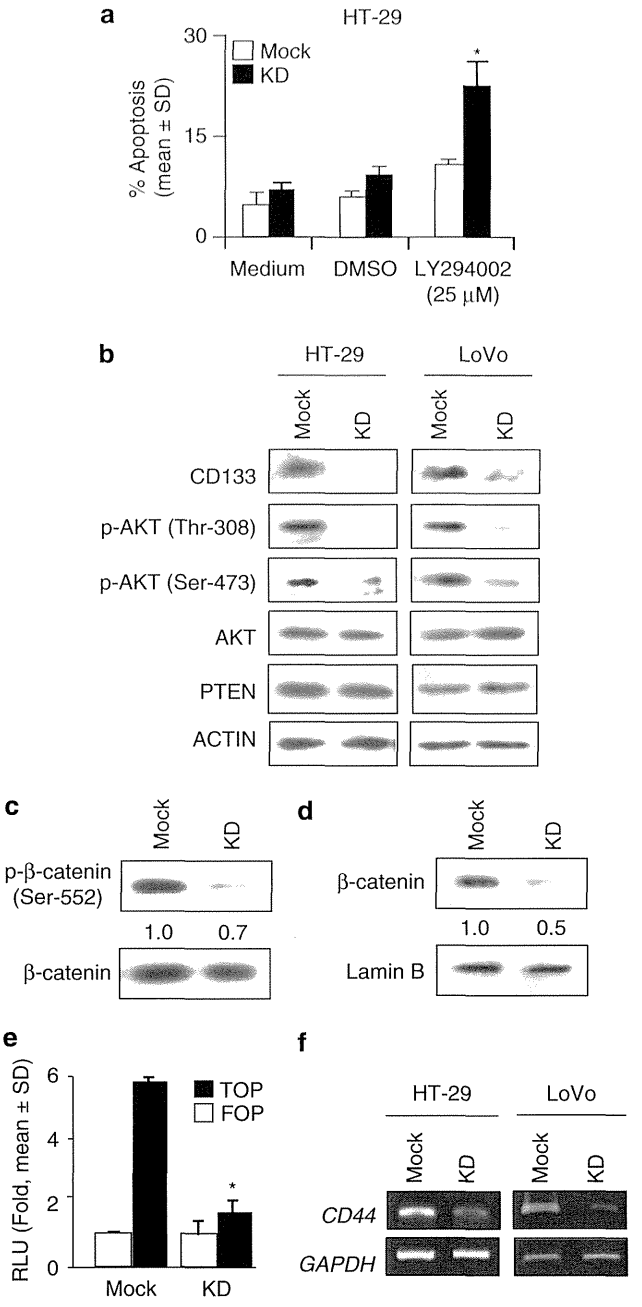

Tyrosine phosphorylation of CD133 promotes xenograft tumor formation through activation of the PI3K/AKT pathway

Boivin *et al.*[26] described that Src family kinases phosphorylate CD133 at tyrosine-828 and tyrosine-852, and also suggested that these tyrosine residues might be involved in CD133 signaling, such as docking for SH2 domain-containing adaptor proteins. As shown in Figure 3a, tyrosine phosphorylation of endogenous CD133 was induced in HT-29 cells exposed to epidermal growth factor (EGF), which could activate Src kinase.[36] To address whether CD133 function could be modulated by its tyrosine phosphorylation, we established other colon cancer-derived SW480 cells expressing mutant forms of CD133, in which tyrosine residues were substituted by phenylalanine (CD133-FF) or glutamate (CD133-EE), and investigated AKT phosphorylation. Of note, endogenous *CD133* transcription was repressed by DNA methylation in SW480 cells (data not shown). Immunoprecipitation–immunoblot experiments demonstrated that other tyrosine residues in CD133-FF and CD133-EE were not phosphorylated in SW480 cells (Figure 3b). We then examined whether wild-type CD133 (CD133-WT)-, CD133-FF- or CD133-EE-expressing SW480 cells could undergo cell death in the presence of LY294002.

Figure 2. CD133 activates the AKT/β-catenin pathway and induces its target CD44 expression. (**a**) Cell death induced by LY294002. CD133-KD and mock-transduced (Mock) HT-29 cells were treated for 24 h with LY294002 and its vehicle control (dimethylsulfoxide (DMSO)). The percentage of apoptosis was measured by flow cytometry. Data are the mean ± s.d. of triplicate. Asterisks indicate the significance of the difference between CD133-KD cells and Mock cells ($P < 0.01$, *t*-test). (**b**) Phosphorylation of AKT in CD133-KD cells. Knockdown of CD133 with HT-29 and LoVo cells was performed as described in the Materials and methods section. Total cell lysates (30 μg) of Mock and CD133-KD cells were subjected to immunoblot analysis for CD133, phosphorylated AKT (p-AKT) at threonine-308 (Thr-308) and serine-473 (Ser-473), AKT, PTEN and ACTIN. (**c**) Phosphorylation of β-catenin in CD133-KD cells. Total cell lysates (20 μg) of Mock and CD133-KD HT-29 cells were subjected to immunoblot analysis for β-catenin and phosphorylated-β-catenin (p-β-catenin) at serine-552 (Ser-552). Relative intensity of phosphorylation is indicated under the image. (**d**) Nuclear accumulation of β-catenin in CD133-KD cells. Nuclear lysates (20 μg) derived from Mock and CD133-KD (KD) HT-29 cells were subjected to immunoblot analysis for β-catenin and lamin B as a loading control. Relative intensity of phosphorylation is indicated under the image. (**e**) Transactivation by β-catenin/TCF complex. Mock and CD133-KD HT-29 cells were transfected with reporter vectors bearing the TCF-driving promoter (TOP) or mutated promoter (FOP). Luciferase activity was measured 48 h after transfection. Data are the mean ± s.d. of triplicate. Asterisk indicates the significance of the difference between CD133-KD cells and Mock cells ($P < 0.05$, *t*-test). (**f**) Expression of *CD44* in CD133-KD cells. *CD44* expression in Mock and CD133-KD cells of HT-29 and LoVo cells was analyzed by semiquantitative RT–PCR.

As shown in Figure 3c, forced expression of CD133-WT rendered the cells resistant to LY294002-induced cell death. CD133-EE-expressing cells were much more resistant to LY294002-induced cell death than CD133-WT-expressing cells, whereas CD133-FF-expressing cells were much more sensitive to LY294002-dependent cell death than mock-transduced cells. In good agreement with these results, forced expression of CD133-WT augmented the phosphorylation level of AKT, whereas the expression level of PTEN remained unchanged (Figure 3d and Supplementary Figure S3). Of note, AKT was highly phosphorylated in CD133-EE-expressing cells as compared with CD133-WT-expressing cells, whereas CD133-FF had a negligible effect on AKT phosphorylation (Figure 3d).

We next examined whether the tyrosine phosphorylation status of CD133 could affect xenograft tumor formation and *in vitro* sphere growth. SW480 cells expressing CD133-WT, CD133-EE or CD133-FF were subcutaneously inoculated into nude mice, and tumors were measured at the indicated time after inoculation. Forced expression of CD133-WT resulted in marked tumor development, whereas CD133-FF-expressing and mock-transduced cells did not form tumors (Figure 3e). In contrast, CD133-EE-expressing cells displayed much more aggressive tumor growth than CD133-WT-expressing cells (Figure 3e). Consistent with these observations, spheroids derived from CD133-WT-expressing cells were significantly larger than those derived from mock-transduced cells and CD133-FF-expressing cells (Figure 3f; $P=0.0001$, ANOVA), whereas CD133-EE-expressing cells formed the largest spheroid (Figure 3f; $P=0.001$, ANOVA). These data collectively suggested that tyrosine phosphorylation of CD133 is

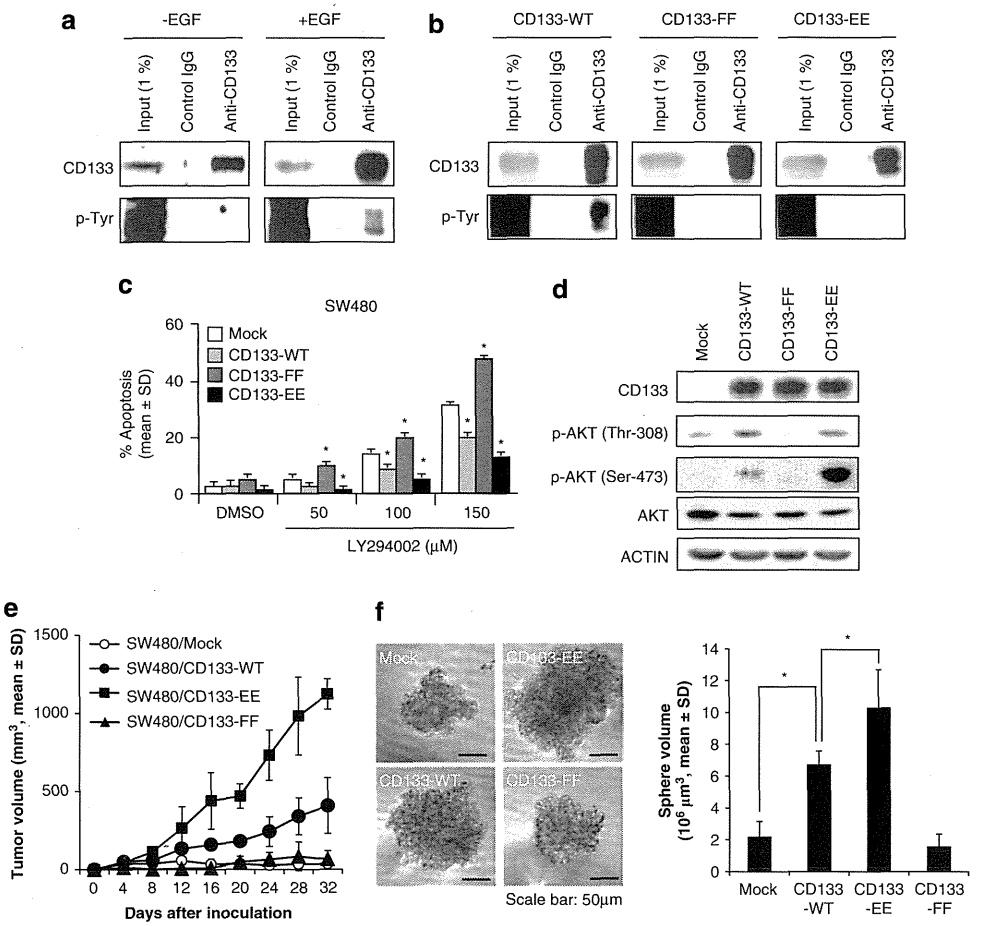

Figure 3. Tyrosine phosphorylation of CD133 triggers PI3K/AKT pathway activation and elevates xenograft tumor formation of colorectal cancer cells. (**a**) Tyrosine phosphorylation of endogenous CD133. HT-29 cells were treated with EGF (20 ng/ml). Total cell lysates were incubated with anti-CD133 monoclonal antibody or control mouse IgG and then precipitated with protein G-Sepharose. Immunoprecipitants were subjected to immunoblot analysis for CD133 and phosphorylated-tyrosine (p-Tyr) residues. (**b**) Tyrosine phosphorylation of mutant CD133. SW480 cells were transfected with *CD133-WT*, *CD133-FF* or *CD133-EE* gene. Total cell lysates were subjected to immunoprecipitation and immunoblot analysis for CD133 and phosphorylated-tyrosine (p-Tyr) residues as described above. (**c**) Cell death induced by LY294002. SW480 cells transduced with mock, *CD133-WT*, *CD133-FF* or *CD133-EE* gene were treated for 24 h with LY294002 and its vehicle control (dimethylsulfoxide (DMSO)). The percentage of apoptosis was measured by flow cytometry. Data are the mean ± s.d. of triplicate. Asterisks indicate the significance of the difference between mock-transduced (Mock) cells and either CD133-WT-, CD133-FF- or CD133-EE-expressing cells ($P < 0.01$, ANOVA). (**d**) Phosphorylation of AKT in mutant CD133-expressing cells. SW480 cells were transduced with *CD133-WT*, *CD133-FF* or *CD133-EE* gene. Total cell lysates (30 μg) of Mock, CD133-WT-, CD133-FF- and CD133-EE-expressing cells were subjected to immunoblot analysis for CD133, phosphorylated AKT (p-AKT) at threonine-308 (Thr-308) and serine-473 (Ser-473), AKT and ACTIN. (**e**) Xenograft tumor growth. Cells (5×10^6 cells) were subcutaneously inoculated into the flanks of BALB/c nude mice ($n=3$). Tumor volumes of Mock (open circles), CD133-WT-expressing (closed circles), CD133-EE-expressing (closed squares) and CD133-FF-expressing (closed triangles) cells on the indicated days show the mean ± s.d. (**f**) Spheroid growth. Cells (10 cells in each well) were cultured for 7 days with serum-free conditioned medium and images of spheroids were obtained. Representative images are shown, and the volume of spheroids calculated by orthogonal diameters is the mean ± s.d. ($n=5$). Asterisks indicate the significance of the difference between Mock cells and CD133-WT-, CD133-FF- or CD133-EE-expressing cells ($P < 0.001$, ANOVA).

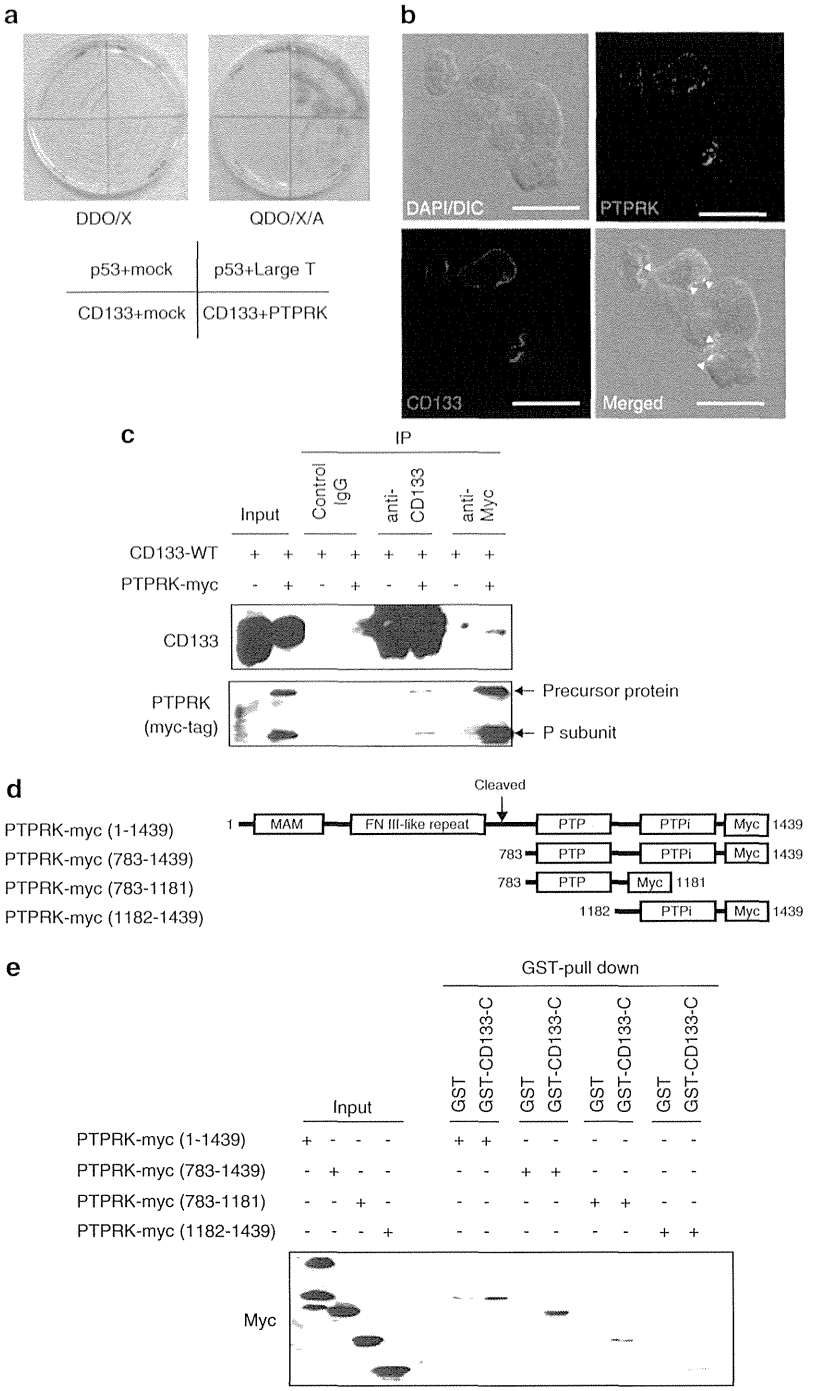

Figure 4. PTPRK binds to CD133. (**a**) A yeast two-hybrid screen. Expression plasmids for bait and prey genes were co-transfected into Y2HGold yeast, and the transfected yeast grew on the selected media without leucine and tryptophan (DDO). Expressions of the four reporter genes, which were driven by the GAL4 transcription factor when the bait protein interacted with the prey protein, were confirmed by blue colony formation on selected media containing aureobasidin A and X-α-gal, but without leucine, tryptophan, histidine and adenine (QDO/X/A). Yeast expressing p53 and large T antigen and that expressing p53 and lamin B were used as positive and negative controls for the interaction between bait and prey, respectively. (**b**) Subcellular localization of CD133 and PTPRK. Caco-2 cells were stained with 4',6-diamidino-2-phenylindole (DAPI) and antibodies against PTPRK and CD133. Fluorescent image was taken by confocal fluorescence microscopy (magnification: x400). White arrowheads indicate merged area. Scale bars = 20 μm. (**c**) Interaction between CD133 and PTPRK in cells. *CD133* and *PTPRK-myc* genes were transfected into 293T cells. Cell lysates were subjected to immunoprecipitation (IP) and immunoblotting with anti-CD133 (CD133) and anti-myc-tag (Myc) antibodies. Precursor PTPRK-myc protein was cleaved in 293T cells and the resultant myc-tagged C-terminal intracellular subunit (P-subunit) was also detected by anti-myc antibody. (**d**) Domain structure of WT PTPRK-myc and schematic representation of the deletion mutants. FN, fibronectin III-like domain; Ig, immunoglobulin-like domain; MAM, meprin/A5/m domain; PTP, active protein tyrosine phosphatase domain; PTPi, inactive protein tyrosine phosphatase domain. Numbers indicate amino-acid positions. (**e**) *In vitro* pull-down assay. GST-CD133-C or GST was incubated with either WT or truncated mutant PTPRK-myc protein. After incubation, GST or GST-CD133-C fusion protein was recovered by glutathione-Sepharose beads, and bound materials were subjected to immunoblotting with anti-myc-tag antibody (Myc).

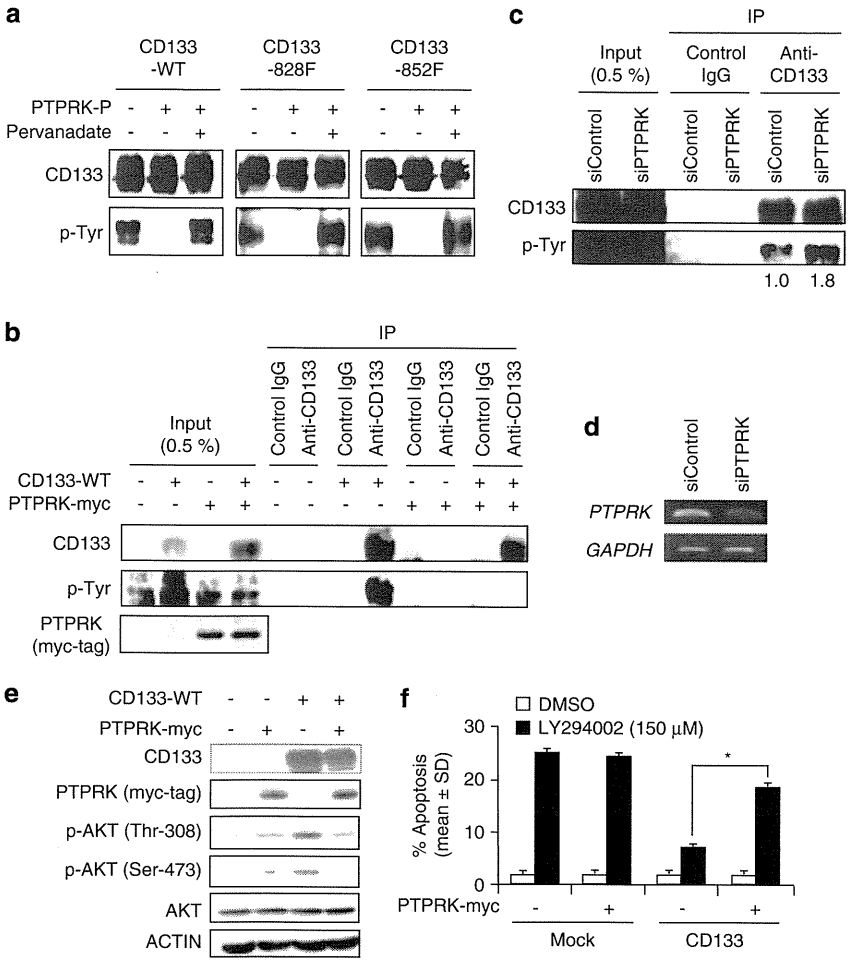

Figure 5. PTPRK dephosphorylates and negatively regulates CD133 signaling. (**a**) *In vitro* phosphatase assay. The 293T cells were transiently transfected with the *CD133-WT*, *CD133-828F* or *CD133-852F* gene and were treated for 15 min with pervanadate 24 h after transfection. Immunoprecipitated CD133 was incubated with PTPRK catalytic domain (PTPRK-P) in the presence or absence of pervanadate *in vitro*. Samples were subjected to immunoblot analysis for CD133 and phosphorylated-tyrosine residues (p-Tyr). (**b**) Phosphorylation of CD133 in PTPRK-expressing cells. Expression plasmids for CD133 and PTPRK-myc were co-transfected into 293T cells. Cell lysates were immunoprecipitated by anti-CD133 antibody. Samples were separated by sodium dodecyl sulfate–polyacrylamide gel electrophoresis (SDS–PAGE) followed by immunoblotting for CD133 and anti-phospho-tyrosine (p-Tyr). (**c** and **d**) Phosphorylation of CD133 in PTPRK-KD cells. A small interfering RNA against *PTPRK* (siPTPRK) or control small interfering RNA (siControl) was transfected into CD133-expressing 293T cells. Cell lysates were immunoprecipitated by anti-CD133 antibody and were immunoblotted by anti-CD133 (CD133) and anti-phosphorylated-tyrosine (p-Tyr) antibodies. Knockdown of PTPRK was determined by semiquantitative RT–PCR in (**d**). (**e**) Phosphorylation of AKT in CD133- and PTPRK-expressing cells. SW480 cells were transduced with *CD133-WT*, *PTPRK-myc* or *CD133-WT* plus *PTPRK* genes. Total cell lysates (30 μg) of mock-transduced (Mock), CD133-WT-, CD133-FF- and CD133-EE-expressing cells were subjected to immunoblot analysis for CD133, PTPRK, phosphorylated AKT (p-AKT) at threonine-308 (Thr-308) and serine-473 (Ser-473), AKT and actin. (**f**) Cell death induced by LY294002 in CD133-expressing SW480 cells. Expression plasmid for PTPRK-myc was transfected into CD133-expressing (CD133) or mock-transducing SW480 (Mock) cells and then treated for 24 h with 150 μM LY294002 or its vehicle control (dimethylsulfoxide (DMSO)). The percentage of apoptosis was measured by flow cytometry. Data are the mean ± s.d. of triplicate. Asterisks indicate the significance of the difference between PTPRK-expressing SW480/CD133 cells and mock-transduced SW480/CD133 cells ($P < 0.01$, *t*-test).

required for the CD133-dependent tumorigenesis of colon cancer cells via activation of the PI3K/AKT/β-catenin signaling pathway.

PTPRK binds to the carboxyl-terminal intracellular domain of CD133 through its phosphatase domain

To identify cellular proteins with the ability to modulate tyrosine phosphorylation of CD133, we used a yeast two-hybrid screening system. For this purpose, we used the carboxyl-terminal intracellular domain of CD133 (CD133-C) as bait to screen the cDNA library derived from the human brain. After extensive screening, we finally obtained six positive candidate clones (data not shown). Sequence analysis revealed that one clone, termed OS-6, encodes PTPRK. As shown in Figure 4a, simultaneous introduction of the bait plasmid and OS-6 plasmid into yeast cells generated blue colonies.

As described previously,[37–40] *PTPRK* encodes a 210 kDa precursor protein belonging to the receptor-type protein tyrosine phosphatase family, which is converted by furin to a mature heterodimeric protein composed of a non-covalently attached amino-terminal extracellular subunit (E-subunit, 120 kDa) and carboxyl-terminal transmembrane subunit (P-subunit, ~95 kDa). Consistent with the previous observation,[40] our indirect immunostaining experiments demonstrated that endogenous PTPRK was expressed predominantly at the sites of cell–cell contact and also colocalized with endogenous CD133 in human colon cancer-derived Caco-2 cells (Figure 4b, arrowheads), indicating that PTPRK might interact with CD133 in mammalian cells. To further

address this issue, cell lysates prepared from 293T cells expressing exogenous CD133 and myc-tagged PTPRK (PTPRK-myc) were immunoprecipitated with control immunoglobulin G (IgG), anti-CD133 or with anti-myc antibody, followed by immunoblotting with the indicated antibodies. Previous studies demonstrated that protein tyrosine phosphatases dissociate immediately from their substrates after catalyzing their dephosphorylation;[41–43] however, both the precursor protein and P-subunit of PTPRK-myc were detected in anti-CD133 immunoprecipitates, and CD133 was co-immunoprecipitated with PTPRK-myc (Figure 4c). Our additional co-immunoprecipitation experiments demonstrated that PTPRK binds to CD133, regardless of its tyrosine phosphorylation status (Supplementary Figure S4). We then sought to determine the regions of the P-subunit of PTPRK (PTPRK-P) required for the interaction with CD133 using an *in vitro* pull-down assay. To this end, we generated a series of PTPRK-myc deletion mutants, including PTPRK-myc (1–1439), PTPRK-myc (783–1439), PTPRK-myc (783–1181) and PTPRK-myc (1182–1439) (Figure 4d). Consistent with the results obtained from our co-immunoprecipitation experiments, the precursor PTPRK-myc (1–1439), PTPRK-myc (783–1439), PTPRK-myc (783–1181) and PTPRK-myc (1182–1439) were efficiently pulled down with glutathione S-transferase (GST)-fused C-terminal portion of CD133 (GST-CD133-C) (Figure 4e), implying that both the intracellular phosphatase domains are important for interaction with the intracellular domain of CD133 (Figure 4e).

PTPRK negatively regulates CD133 function via tyrosine dephosphorylation

Our present results, showing the interaction of PTPRK with CD133 through its phosphatase domain, prompted us to examine whether PTPRK could directly dephosphorylate CD133. For this purpose, we used an *in vitro* phosphatase assay using PTPRK-P[40] and mutant forms of CD133, of which tyrosine residue at 828 (CD133-828F) or 852 (CD133-852F) was substituted by phenylalanine. Notably, CD133-FF was not phosphorylated in 293T cells, implying that only these tyrosine residues are phosphorylated (Supplementary Figure S5). The 293T cells were transiently transfected with the expression plasmid for CD133-WT, CD133-828F or CD133-852F and then these proteins were purified by immunoprecipitation. Purified CD133 proteins were incubated with PTPRK-P in the presence or absence of a protein tyrosine phosphatase-specific inhibitor, pervanadate. As seen in Figure 5a, incubation with PTPRK-P led to a marked reduction of the phosphorylation level of purified CD133 at tyrosine-828 and tyrosine-852 *in vitro*, whereas pervanadate treatment blocked PTPRK-P-mediated tyrosine dephosphorylation of purified CD133. For further confirmation, 293T cells were transfected with the indicated combinations of the expression plasmids, and cell lysates were immunoprecipitated with control IgG or anti-CD133 antibody, followed by immunoblotting with the indicated antibodies. As shown in Figure 5b, the anti-CD133 immunoprecipitates derived from 293T cells transfected with CD133 alone contained a large amount of CD133 phosphorylated at tyrosine residues, whereas coexpression of CD133 and PTPRK resulted in marked reduction in the amounts of tyrosine-phosphorylated CD133 (Figure 5b), indicating that PTPRK has the ability to dephosphorylate CD133. In support of these observations, small interfering RNA-mediated knockdown of endogenous PTPRK led to significant enhancement of the tyrosine phosphorylation of CD133 (Figures 5c and d). We then examined the biological consequences of CD133/PTPRK interaction. For this purpose, SW480 cells were transfected with the expression plasmid for PTPRK, CD133, or with the expression plasmids encoding PTPRK plus CD133, and their AKT phosphorylation status was examined. As seen in Figure 5e, PTPRK diminished the increase in AKT phosphorylation of CD133-expressing cells. In addition, forced expression of CD133 inhibited LY294002-induced cell death, whereas SW480 cells expressing CD133 plus PTPRK underwent cell death in response to LY294002 (Figure 5f; $P=7.8\times10^{-7}$, *t*-test), suggesting that PTPRK attenuates the functions of CD133.

Expression levels of CD133 and PTPRK are related to the prognosis of colon cancer patients with tumor recurrence

We next examined the possible clinical significance of CD133 and PTPRK in colon cancer patients. Expression levels of putative CSC markers such as epithelial cell adhesion molecule (EpCAM), CD44, CD133[44] and phosphorylated AKT in primary colon cancer-derived cells were examined by flow cytometry. EpCAM and CD44 double-positive ($EpCAM^+CD44^+$) cells were a major subset in colon cancer tissues but not in their adjacent normal mucosal tissues (Supplementary Figure S6a). Some $EpCAM^+CD44^+$ cells expressed CD133, whereas CD133 was hardly detectable in normal mucosal cells (Supplementary Figure S6b). The percentage of phosphorylated AKT-positive cells was significantly higher in $EpCAM^+CD44^+CD133^+$ cells than in $EpCAM^+CD44^+CD133^-$ cells ($P=0.0288$, $n=6$, paired *t*-test; Figures 6a and b). CD44 expression was also significantly higher in EpCAM and CD133 double-positive cells than in EpCAM single-positive cells ($P=0.0297$, $n=6$, paired *t*-test; Figures 6c and d). To confirm these observations, we transduced the *CD133* gene into primary cells derived from colon cancer patients using a lentiviral vector. Ectopic expression of CD133 in primary cultured cancer cells showed an increase in AKT phosphorylation (Figure 6e).

We finally assessed whether PTPRK could be used as a prognostic factor in colon cancer. Kaplan–Meier analysis using two independent public microarray data sets revealed significant correlation between short relapse-free survival (RFS) and the low expression of *PTPRK* in all patients (Figure 6f). To investigate the potential impact of CD133/PTPRK interaction in colon cancer, the correlation between RFS and the expression level of *PTPRK* was analyzed using patients classified by the expression level of *CD133*. Low expression of *PTPRK* might indicate a poor prognosis of patients with higher expression of *CD133* than its average, whereas RFS was not correlated with the expression level of *PTPRK* of patients with low expression of *CD133* (Figure 6g). To further investigate the potential impact of CD133/PTPRK interaction in advanced colon cancer, RFS of patients with recurrent tumor was analyzed, classified by expression levels of CD133 and *PTPRK*. We found that short RFS is closely associated with high expression of *CD133* or with low expression of *PTPRK* in patients with recurrent tumor (Figure 6h).

DISCUSSION

Several lines of evidence suggest that CD133 might be a strong candidate for a CSC marker.[16–19] Unfortunately, large amounts of these previous studies used a certain population of tumor cells purified from primary tumors based on the expression level of CD133; therefore, it appears to be difficult to exclude completely the possibility of the intrinsic tumor-initiating ability of $CD133^-$ tumor cells.[45,46] To understand precisely the tumorigenic property of CD133 in detail, extensive experiments such as knockdown and/or forced expression of CD133 in tumor-derived cell lines with a homogenous cellular background are required. Intriguingly, Wei *et al.*[47] recently described that the phosphorylation level of CD133 is strongly associated with the progression of human glioma. Consistent with these observations, we found for the first time that the tyrosine phosphorylation of CD133 directly promotes tumorigenesis and the sphere growth of human colon cancer-derived cell lines through activation of the AKT/β-catenin oncogenic pathway (Figure 7). Previous reports demonstrated that colorectal CSCs express an extremely low level of PTEN; therefore, the PI3K/AKT pathway might be constitutively activated in colorectal CSCs.[48,49]

Our present results show that the ectopic expression of CD133 enhances AKT phosphorylation in established colon cancer cell lines as well asin freshly prepared primary colon cancer-derived cells, which expressed modest amounts of PTEN. In this regard, it appears that a critical issue was adequately addressed as to whether overexpression of CD133 could regulate the PI3K/AKT pathway in PTEN-depleted primary colon cancer cells.

We have also found that EGF stimulates the phosphorylation of CD133. It is well known that EGF/EGFR signaling activates numerous pro-oncogenic pathways to promote tumor growth, including PI3K/AKT, Ras/MAPK and Src kinase. Among them, Src kinase activity was enhanced during the progression of colorectal cancer;[50] thus, it is likely that Src kinase activity is an indicator of the poor prognosis of colorectal cancer patients.[51] In good agreement with these findings, Chen *et al.*[52] described that the expression level of CD133 is concordant with the activation of Src in human head and neck cancer cells, implying that CD133 might augment the activity of Src. Based on our present results, CD133 was detected in a small population of primary colon cancer cells, which might contain putative colon CSCs. Thus, precise understanding of the aberrant activation of the EGF/CD133/Src axis might provide a clue to develop a novel strategy for CSC-targeted therapy.

Another novel finding of the present study was that PTPRK directly dephosphorylates CD133. Several lines of evidence suggested that *PTPRK* acts as a putative tumor suppressor gene

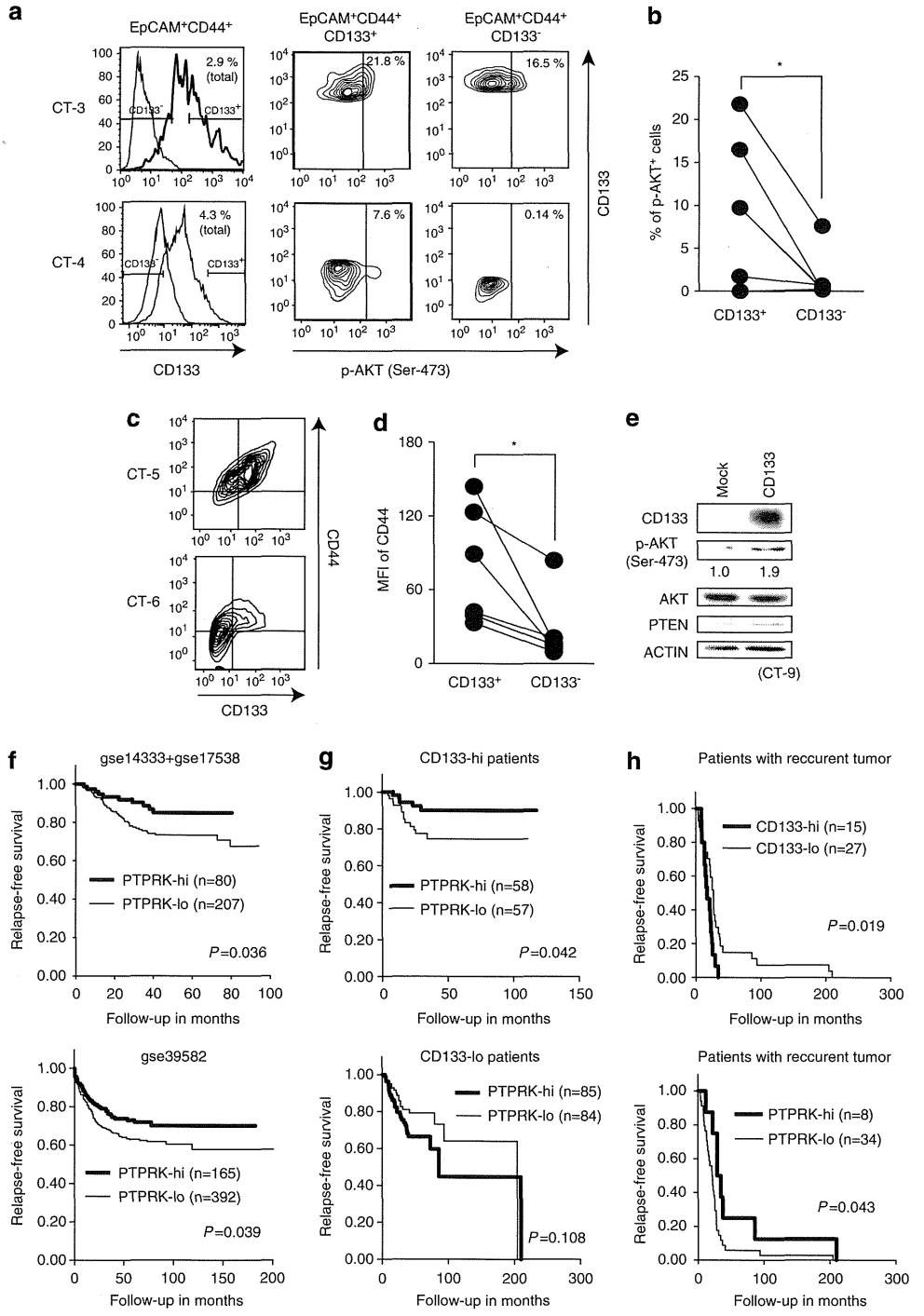

for colorectal cancer. For example, an association has been shown between loss of heterogeneity at *PTPRK*, including the locus and the early onset of hereditary intestinal carcinomas,[53] and transgenic mice harboring transposon-mediated deletion of *Ptprk in gastrointestinal epithelium, which exhibit an increase in* susceptibility to intestinal tumorigenesis.[54] Our present results have demonstrated that loss of tyrosine phosphorylation suppresses the pro-oncogenic function of CD133. From the clinical point of view, low expression of *PTPRK* was correlated with the poor prognosis of colon cancer patients with high expression of *CD133*, suggesting that PTPRK might abrogate the ability of CD133 to accelerate the tumor progression of colon cancer (Figure 7). PTPRK also catalyzed tyrosine dephosphorylation of β-catenin, which regulates its transactivating activity.[40,55] Mak *et al.*[56] recently described that CD133 physically associates with β-catenin, thereby activating β-catenin through its deacetylation by HDAC6. Taken together, it is likely that PTPRK has a pivotal role in the regulation of CD133-mediated pro-oncogenic pathways through the suppression of PI3K/AKT and/or β-catenin.

In conclusion, we have found that CD133 has a crucial role in colon carcinogenesis via its tyrosine phosphorylation followed by subsequent activation of the AKT-β-catenin oncogenic pathway. Furthermore, we identified PTPRK as a novel negative regulator of CD133 in colon cancer cells. Thus, our present findings strongly suggest that PTPRK-mediated attenuation of CD133 might provide a clue to develop a novel strategy for CSC-targeted therapy.

MATERIALS AND METHODS

Cell culture and transfection

Human colon carcinoma-derived HT-29, LoVo and SW480 cells were obtained from ATCC (Manassas, VA, USA) and Caco-2 cells were received from the RIKEN Bioresource Center (Ibaraki, Japan). All cell lines were verified by short tandem repeat analysis. Cells were cultured with Dulbecco's modified Eagle's medium (Wako Pure Chemical Industries, Osaka, Japan) supplemented with 10% heat-inactivated fetal bovine serum (Invitrogen, Carlsbad, CA, USA) and 50 μg/ml penicillin/streptomycin (Sigma-Aldrich, St Louis, MO, USA) in a humidified atmosphere with 5% CO_2 at 37 °C. Transfections were performed using FuGENE HD reagent (Promega, Madison, WI, USA).

Construction of mutant CD133-expressing vector

Mutant *CD133*, whose tyrosine-828, tyrosine-852 and tyrosine-828/852 residues were substituted by phenylalanine (*CD133-828F*, *CD133-852F* and *CD133-FF*) or glutamate (*CD133-EE*), and were generated using the

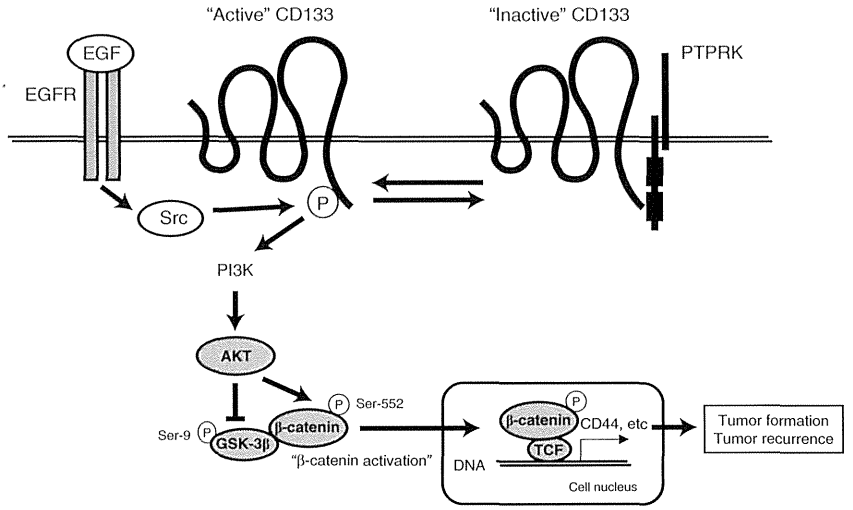

Figure 7. Summary of the present study.

Figure 6. CD133 and PTPRK expression is related to the prognosis of colon cancer patients with tumor recurrence. (**a**) Representative pattern of AKT phosphorylation in $CD133^+$ primary colon cancer cells. Colon cancer tissues were enzymatically digested as described in the Materials and Methods section. Cells were stained with anti-EpCAM, anti-CD44, anti-CD133 and anti-phosphorylated-AKT (p-AKT) at serine-473 (Ser-473) antibodies. CD133 expression in EpCAM and CD44 double-positive ($EpCAM^+CD44^+$) cells are shown in left panels (bold line) and the percentage of $CD133^+$ ($CD133^+$) cells in $EpCAM^+CD44^+$ cells is shown in right upper corners of each panel. Representative patterns of p-AKT in $EpCAM^+CD44^+$-gated $CD133^+$ or $CD133^-$ cells are shown in middle and right panels, respectively. The percentage of p-AKT-positive ($p\text{-}AKT^+$) cells is shown in the right upper corner of each panel. (**b**) Percentage of $p\text{-}AKT^+$ cells. Data from six colon cancer patients are shown. Asterisk indicates the significance of the difference between $CD133^+$ and CD133 − cells ($P < 0.05$, $n = 6$, paired *t*-test). (**c**) CD44 and CD133 expressions in primary colon cancer cells. CD44 and CD133 expressions in $EpCAM^+$ cells are shown. (**d**) Mean fluorescence intensity (MFI) of CD44 expression. Data from six colon cancer patients are shown. Asterisk indicates the significance of the difference between $CD133^+$ and $CD133^-$ cells ($P < 0.05$, $n = 6$, paired *t*-test). (**e**) Phosphorylation of AKT in CD133-expressing primary colon cancer cells. Primary colon cancer-derived cells were transduced with the *CD133* gene. Total cell lysates (15 μg) of mock-transduced and CD133-WT-expressing cells were subjected to immunoblotting for CD133, phosphorylated AKT (p-AKT) at threonine-308 (Thr-308) and serine-473 (Ser-473), AKT and ACTIN. (**f**) RFS of colon cancer patients. Kaplan–Meier survival analysis was performed using two independent public microarray data sets (gse14333 plus gse17538 and gse39582) as described in the Materials and methods section. RFS probabilities of colon cancer patients with high and low expressions of *PTPRK* are shown. The cutoff value was determined automatically by an online tool (http://r2.amc.nl). (**g**) RFS probabilities of the patients with high and low expressions of *CD133* and *PTPRK*. Kaplan–Meier survival analysis was performed as described above. The patients enrolled in the data set (gse14333 plus gse17538) were categorized by their expression level of *CD133*: The cutoff value is the average *CD133* in this data set. RFS probabilities of each group with high and low expressions of *PTPRK* are shown: the cutoff value is the median value of *PTPRK* expression. (**h**) RFS of colon cancer patients with recurrent tumor. Patients with recurrent tumor were extracted from the public microarray data set (gse14333 plus gse17538) and then Kaplan–Meier survival analysis was performed as described in (**e**). The cutoff value was determined automatically by an online tool (http://r2.amc.nl).

QuikChange II Site-Directed Mutagenesis Kit (Agilent Technology, Santa Clara, CA, USA), with the primers listed in Supplementary Table S1. Each sequence-confirmed mutant gene or *CD133-WT* gene was subcloned into an expression vector (pcDNA3; Invitrogen) and also into a lentivirus-transducing vector (pCDH-CMV-MCS-EF1-puro; System Bioscience, Mountain View, CA, USA).

Lentivirus-mediated transduction of short hairpin RNA and mutant CD133

Lentiviral particles bearing short hairpin RNA against *CD133* or mutant CD133 were produced by transducing and packaging vectors (MISSION Lentiviral Packaging Mix; Sigma-Aldrich) as described previously.[27,57]

Analysis of RNA expression

Total RNA extraction, first-strand DNA synthesis and semiquantitative reverse transcription–polymerase chain reaction (RT–PCR) were performed as described previously.[58] Primer sequences and conditions of PCR amplification are shown in Supplementary Table S1.

Xenograft tumor experiments

Cells were inoculated subcutaneously into BALB/c nude mice (CREA Japan, Shizuoka, Japan) as described previously.[27] The handling of animals was in accordance with the guidelines of Chiba Cancer Center Research Institute, Chiba, Japan.

Soft agar colony formation

Soft agar colony formation assay was carried out as described previously.[27]

Sphere growth assay

Ten cells were cultured for 7 days in a low-adherent round-bottomed 96-well plate (Sumitomo Bakelite, Tokyo, Japan) with sphere-forming medium, consisting of Dulbecco's modified Eagle's medium/F-12 supplemented with 2% B27 plus (Miltenyi Biotech, Auburn, CA, USA), 20 ng/ml EGF (R&D Systems, Minneapolis, MN, USA) and 20 ng/ml fibroblast growth factor-2 (Miltenyi Biotech). Images were captured using a microscope and analyzed with ImageJ digital imaging software (Rasband, W.S., ImageJ, U.S. National Institute of Health, Bethesda, MD, USA, http://imagej.nih.gov/ij/, 1997-2014). The volume (*V*) was calculated with the following formula: $V = 4/3\pi \times (\text{long diameter}) \times (\text{short diameter})^2$.

Immunoblot analysis

Cells were lysed with a lysis buffer containing 50 mM Tris-HCl (pH 7.5), 150 mM NaCl, 0.5% Triton X-100 and 1 mM EDTA, protease inhibitor cocktail (Calbiochem, San Diego, CA, USA) and phosphatase inhibitor cocktail (Roche Applied Science, Indianapolis, IN, USA). Nuclei of cells were isolated using the ProteoExtract subcellular proteome extraction kit (Calbiochem). The resultant cell lysates were subjected to immunoblotting as described previously.[27] Membranes were probed with antibodies: myc-tag, β-catenin, phospho-β-catenin at serine-552, AKT, phospho-AKT at serine-473 and threonine-308, GSK-3β, phospho-GSK-3β at serine-9, phosphotyrosine, horseradish peroxidase-conjugated anti-mouse IgG and horseradish peroxidase-conjugated anti-rabbit IgG (all Cell Signaling Technology, Beverly, MA, USA), actin (Sigma-Aldrich), CD133 (Miltenyi Biotech) and PTEN (Santa Cruz Biotechnology, Santa Cruz, CA, USA) and were visualized by an ImageQuant LAS4000mini imager (GE Healthcare Bioscience, Pittsburgh, PA, USA).

Immunoprecipitation and immunoblot analysis

Immunoprecipitation and immunoblotting were performed as described previously.[59] For the analysis of protein tyrosine phosphorylation, $CD133^+$ HT-29 cells were incubated for 30 min with 20 ng/ml EGF (R&D Systems) and $CD133^-$ cells (SW480 and 293T) were transiently transfected with expression plasmids for *CD133-WT*, *CD133-EE* and *CD133-FF*. Cells were treated with pervanadate (0.3% (w/w) H_2O_2 and 0.1 mM sodium orthovanadate) and then were solubilized with lysis buffer as described above. Cleared lysates were mixed with an anti-CD133 antibody (Miltenyi Biotech) and protein G-Sepharose beads. Anti-CD133 immunoprecipitates were subjected to immunoblotting with the indicated antibodies. For co-immunoprecipitation analysis, expression plasmids for *CD133* and *PTPRK-myc* were transiently co-transfected into 293T cells. Protein extraction, immunoprecipitation and immunoblotting were carried out as described above.

GST pull-down assay

The GST pull-down assay was performed as described previously.[59] cDNA encoding the CD133-C (816–865 amino acids (aa)) was generated by PCR using the primers listed in Supplementary Table S1 and subcloned into pGEX-4T-1 vector (GE Healthcare Bioscience) and was transformed into *Escherichia coli*. GST-CD133-C and GST were purified using glutathione-Sepharose beads (50% slurry; GE Healthcare Bioscience). cDNAs encoding full-length *PTPRK* and a truncated form of *PTPRK*, the carboxyl-terminal domain (783–1439 aa), active phosphatase domain (783–1181 aa) and inactive phosphatase domain (1182–1439 aa), were generated by a PCR-based method with the primers listed in Supplementary Table S1 and were subcloned into pcDNA3-myc-His-A vector (Invitrogen). The 293T cells were transfected with plasmid DNA bearing WT *PTPRK* or each mutant *PTPRK* cDNA and then were solubilized with lysis buffer as described above. The protein extracts bound to GST-CD133-C or GST were separated by sodium dodecyl sulfate–polyacrylamide gel electrophoresis and detected by immunoblotting.

Luciferase reporter gene assay

pRL-TK vector (Promega) and either pTOP-FLASH (Millipore, Billerica, MA, USA) or pFOP-FLASH vector (Millipore) were transiently co-transfected into HT-29 cells. Forty-eight hours after transfection, luciferase activities of cell extracts were measured with a Dual Luciferase Kit (Promega).

Yeast two-hybrid screening

Yeast two-hybrid screening was performed as described previously.[60] CD133-C cDNA was generated by PCR using the primers listed in Supplementary Table S1 and cloned into pGBKT7 vector, creating a GAL4-fused 'bait' protein. Bait protein-expressing yeast (Y2HGold; Clontech, Mountain View, CA, USA) was subjected to mating with human fetal brain cDNA library-expressing yeast (Y187; Clontech).

Immunofluorescence staining

Caco-2 cells were grown on glass coverslips and stained with anti-PTPRK antibody (Santa Cruz Biotechnology) for 30 min at 4 °C. After extensive washing in PBS, cells were stained with Alexa Fluor 488-conjugated anti-mouse IgG antibody (Invitrogen) for 10 min, followed by phycoerythrin-conjugated anti-CD133 antibody (Miltenyi Biotech) for 30 min. Cells were then fixed with 100% methanol for 10 min at −20 °C. Coverslips were mounted with Prolong Gold Antifade reagent with 4′,6-diamidino-2-phenylindole (Invitrogen). Fluorescence images were observed with a microscope (DMI 4000B; Leica, Wetzlar, Germany).

In vitro dephosphorylation assay

Tyrosine-phosphorylated CD133 was prepared from CD133-expressing 293T cells treated with pervanadate by immunoprecipitation as described above, and then incubated with 50 ng purified hPTPRK (MBL, Nagoya, Japan) as described previously.[40]

Tissue collection and isolation of primary colon cancer cells

Human colon tissues were obtained from patients undergoing colon resection in the Department of Gastrointestinal Surgery, Chiba Cancer Center Hospital (see Supplementary Table S2) in accordance with the ethics standards of the institutional committee. Tissue specimens were enzymatically digested and then cancer tissue-originating spheroids were prepared as described previously.[61] For the analysis of AKT phosphorylation, cancer tissue-originating spheroids were cultured with sphere-forming medium for 3 days and the *CD133* gene was transduced by the lentiviral vector as described above.

Flow cytometry

Cells were stained for 30 min at 4 °C with antibodies: allophycocyanin-conjugated EpCAM (Miltenyi Biotech), phycoerythrin-conjugated CD133 (Miltenyi Biotech), phycoerythrin-Cy5-conjugated CD44 (BioLegend, San Diego, CA, USA) and appropriate isotype control antibodies (e-Bioscience, San Diego, CA, USA). For AKT phosphorylation analysis, cells were stained

with Alexa Fluor 488-conjugated anti-phospho-AKT at serine-473 antibody (Cell Signaling Technology) and antibodies against EpCAM, CD133 and CD44 as described above in accordance with the instructions of the Cytofix/Cytoperm intracellular staining kit (BD Biosciences, Franklin Lakes, NJ, USA). Expression profiles were determined by a FACSCalibur flow cytometer (BD Biosciences) and FlowJo software (Tree Star, Ashland, OR, USA).

Cell death induced by LY294002

Cells were treated with a PI3K inhibitor, LY294002 (Wako Pure Chemical Industries), at the indicated concentrations and hours in each experiment. The cells were harvested and fixed in 100 % ethanol for 24 h at 4 °C and then stained with propidium iodide (50 μg/ml; Sigma-Aldrich) followed by RNaseH treatment (50 μg/ml; Sigma-Aldrich). The percentage of cell death was determined by flow cytometry as described above.

Survival curve generation

Survival data and expression levels of *PTPRK* (probe: 203038) and CD133 (probe: 204304) of colon cancer patients were obtained from two independent microarray data sets (gse39582 and gse14333 plus gse17538). Relapse-free survival is represented as a Kaplan–Meier plot and was statistically investigated with the log-rank test using the R2: Microarray Analysis and Visualization Platform (http://r2.amc.nl).

CONFLICT OF INTEREST

The authors declare no conflict of interest.

ACKNOWLEDGEMENTS

We thank Ms Kumiko Sakurai for technical assistance, Mr Daniel Mrozek (Medical English Service, Kyoto, Japan) for English editorial assistance and Dr Takafumi Nakamura (Graduate School of Medical Sciences, Tottori University Faculty of Medicine) for pHR lentiviral vectors. This work was supported in part by grants-in-aid from JSPS for Young Scientists (B) and for Scientific Research (C) (Grant numbers: 21790397 and 23591978, respectively), a grant-in-aid for Scientific Research (B) from JSPS (24390269) and a grant-in-aid from the National Cancer Center Research and Development Fund (25-B-3).

REFERENCES

1 Siegel R, Ward E, Brawley O, Jemal A. Cancer statistics, 2011: the impact of eliminating socioeconomic and racial disparities on premature cancer deaths. *CA Cancer J Clin* 2011; **61**: 212–236.
2 Cunningham D, Atkin W, Lenz H-J, Lynch HT, Minsky B, Nordlinger B *et al.* Colorectal cancer. *Lancet* 2010; **375**: 1030–1047.
3 Reya T, Morrison SJ, Clarke MF, Weissman IL. Stem cells, cancer, and cancer stem cells. *Nature* 2001; **414**: 105–111.
4 Dean M, Fojo T, Bates S. Tumour stem cells and drug resistance. *Nat Rev Cancer* 2005; **5**: 275–284.
5 Pardal R, Clarke MF, Morrison SJ. Applying the principles of stem-cell biology to cancer. *Nat Rev Cancer* 2003; **3**: 895–902.
6 Yin AH, Miraglia S, Zanjani ED, Almeida-Porada G, Ogawa M, Leary AG *et al.* AC133, a novel marker for human hematopoietic stem and progenitor cells. *Blood* 1997; **90**: 5002–5012.
7 Miraglia S, Godfrey W, Yin AH, Atkins K, Warnke R, Holden JT *et al.* A novel five-transmembrane hematopoietic stem cell antigen: isolation, characterization, and molecular cloning. *Blood* 1997; **90**: 5013–5021.
8 Mizrak D, Brittan M, Alison MR. CD133: molecule of the moment. *J Pathol* 2008; **214**: 3–9.
9 Bussolati B, Bruno S, Grange C, Buttiglieri S, Deregibus MC, Cantino D *et al.* Isolation of renal progenitor cells from adult human kidney. *Am J Pathol* 2005; **166**: 545–555.
10 Uchida N, Buck DW, He D, Reitsma MJ, Masek M, Phan TV *et al.* Direct isolation of human central nervous system stem cells. *Proc Natl Acad Sci USA* 2000; **97**: 14720–14725.
11 Lee A, Kessler JD, Read TA, Kaiser C, Corbeil D, Huttner WB *et al.* Isolation of neural stem cells from the postnatal cerebellum. *Nat Neurosci* 2005; **8**: 723–729.
12 Zhu L, Gibson P, Currle DS, Tong Y, Richardson RJ, Bayazitov IT *et al.* Prominin 1 marks intestinal stem cells that are susceptible to neoplastic transformation. *Nature* 2009; **457**: 603–607.
13 Singh SK, Clarke ID, Hide T, Dirks PB. Cancer stem cells in nervous system tumors. *Oncogene* 2004; **23**: 7267–7273.
14 Bao S, Wu Q, McLendon RE, Hao Y, Shi Q, Hjelmeland AB *et al.* Glioma stem cells promote radioresistance by preferential activation of the DNA damage response. *Nature* 2006; **444**: 756–760.
15 O'Brien CA, Pollett A, Gallinger S, Dick JE. A human colon cancer cell capable of initiating tumour growth in immunodeficient mice. *Nature* 2007; **445**: 106–110.
16 Ricci-Vitiani L, Lombardi DG, Pilozzi E, Biffoni M, Todaro M, Peschle C *et al.* Identification and expansion of human colon-cancer-initiating cells. *Nature* 2007; **445**: 111–115.
17 Miki J, Furusato B, Li H, Gu Y, Takahashi H, Egawa S *et al.* Identification of putative stem cell markers, CD133 and CXCR4, in hTERT-immortalized primary non-malignant and malignant tumor-derived human prostate epithelial cell lines and in prostate cancer specimens. *Cancer Res* 2007; **67**: 3153–3161.
18 Todaro M, Alea MP, Di Stefano AB, Cammareri P, Vermeulen L, Iovino F *et al.* Colon cancer stem cells dictate tumor growth and resist cell death by production of interleukin-4. *Cell Stem Cell* 2007; **1**: 389–402.
19 Vermeulen L, Todaro M, de Sousa Mello F, Sprick MR, Kemper K, Perez Alea M *et al.* Single-cell cloning of colon cancer stem cells reveals a multi-lineage differentiation capacity. *Proc Natl Acad Sci USA* 2008; **105**: 13427–13432.
20 Kojima M, Ishii G, Atsumi N, Fujii S, Saito N, Ochiai A. Immunohistochemical detection of CD133 expression in colorectal cancer: a clinicopathological study. *Cancer Sci* 2008; **99**: 1578–1583.
21 Horst D, Scheel SK, Liebmann S, Neumann J, Maatz S, Kirchner T *et al.* The cancer stem cell marker CD133 has high prognostic impact but unknown functional relevance for the metastasis of human colon cancer. *J Pathol* 2009; **219**: 427–434.
22 Artells R, Moreno I, Diaz T, Martinez F, Gel B, Navarro A *et al.* Tumour CD133 mRNA expression and clinical outcome in surgically resected colorectal cancer patients. *Eur J Cancer* 2010; **46**: 642–649.
23 Nikolova T, Wu M, Brumbarov K, Alt R, Opitz H, Boheler KR *et al.* WNT-conditioned media differentially affect the proliferation and differentiation of cord blood-derived CD133+ cells *in vitro*. *Differ Res Biol Divers* 2007; **75**: 100–111.
24 Fan X, Matsui W, Khaki L, Stearns D, Chun J, Li YM *et al.* Notch pathway inhibition depletes stem-like cells and blocks engraftment in embryonal brain tumors. *Cancer Res* 2006; **66**: 7445–7452.
25 Ma S, Lee TK, Zheng BJ, Chan KW, Guan XY. $CD133^+$ HCC cancer stem cells confer chemoresistance by preferential expression of the Akt/PKB survival pathway. *Oncogene* 2008; **27**: 1749–1758.
26 Boivin D, Labbe D, Fontaine N, Lamy S, Beaulieu E, Gingras D *et al.* The stem cell marker CD133 (prominin-1) is phosphorylated on cytoplasmic tyrosine-828 and tyrosine-852 by Src and Fyn tyrosine kinases. *Biochemistry* 2009; **48**: 3998–4007.
27 Takenobu H, Shimozato O, Nakamura T, Ochiai H, Yamaguchi Y, Ohira M *et al.* CD133 suppresses neuroblastoma cell differentiation via signal pathway modification. *Oncogene* 2011; **30**: 97–105.
28 Dubrovska A, Kim S, Salamone RJ, Walker JR, Maira SM, Garcia-Echeverria C *et al.* The role of PTEN/Akt/PI3K signaling in the maintenance and viability of prostate cancer stem-like cell populations. *Proc Natl Acad Sci USA* 2009; **106**: 268–273.
29 Hu L, Zaloudek C, Mills GB, Gray J, Jaffe RB. *In vivo* and *in vitro* ovarian carcinoma growth inhibition by a phosphatidylinositol 3-kinase inhibitor (LY294002). *Clin Cancer Res* 2000; **6**: 880–886.
30 Uddin S, Hussain AR, Siraj AK, Manogaran PS, Al-Jomah NA, Moorji A *et al.* Role of phosphatidylinositol 3'-kinase/AKT pathway in diffuse large B-cell lymphoma survival. *Blood* 2006; **108**: 4178–4186.
31 Sarbassov DD, Guertin DA, Ali SM, Sabatini DM. Phosphorylation and regulation of Akt/PKB by the rictor–mTOR complex. *Science* 2005; **307**: 1098–1101.
32 Stephens L, Anderson K, Stokoe D, Erdjument-Bromage H, Painter GF, Holmes AB *et al.* Protein kinase B kinases that mediate phosphatidylinositol 3,4,5-trisphosphate-dependent activation of protein kinase B. *Science* 1998; **279**: 710–714.
33 Cantley LC, Neel BG. New insights into tumor suppression: PTEN suppresses tumor formation by restraining the phosphoinositide 3-kinase/AKT pathway. *Proc Natl Acad Sci USA* 1999; **96**: 4240–4245.
34 Fang D, Hawke D, Zheng Y, Xia Y, Meisenhelder J, Nika H *et al.* Phosphorylation of beta-catenin by AKT promotes beta-catenin transcriptional activity. *J Biol Chem* 2007; **282**: 11221–11229.
35 Wielenga VJ, Smits R, Korinek V, Smit L, Kielman M, Fodde R *et al.* Expression of CD44 in Apc and Tcf mutant mice implies regulation by the WNT pathway. *Am J Pathol* 1999; **154**: 515–523.
36 Kraus S, Benard O, Naor Z, Seger R. c-Src is activated by the epidermal growth factor receptor in a pathway that mediates JNK and ERK activation by gonadotropin-releasing hormone in COS7 cells. *J Biol Chem* 2003; **278**: 32618–32630.
37 Anders L, Mertins P, Lammich S, Murgia M, Hartmann D, Saftig P *et al.* Furin-, ADAM 10-, and gamma-secretase-mediated cleavage of a receptor tyrosine phosphatase and regulation of beta-catenin's transcriptional activity. *Mol Cell Biol* 2006; **26**: 3917–3934.

38 Yang Y, Gil MC, Choi EY, Park SH, Pyun KH, Ha H. Molecular cloning and chromosomal localization of a human gene homologous to the murine R-PTP-kappa, a receptor-type protein tyrosine phosphatase. *Gene* 1997; **186**: 77–82.
39 Jiang YP, Wang H, D'Eustachio P, Musacchio JM, Schlessinger J, Sap J. Cloning and characterization of R-PTP-kappa, a new member of the receptor protein tyrosine phosphatase family with a proteolytically cleaved cellular adhesion molecule-like extracellular region. *Mol Cell Biol* 1993; **13**: 2942–2951.
40 Fuchs M, Muller T, Lerch MM, Ullrich A. Association of human protein-tyrosine phosphatase kappa with members of the armadillo family. *J Biol Chem* 1996; **271**: 16712–16719.
41 Xu Y, Xia W, Baker D, Zhou J, Cha HC, Voorhees JJ *et al.* Receptor-type protein tyrosine phosphatase beta (RPTP-beta) directly dephosphorylates and regulates hepatocyte growth factor receptor (HGFR/Met) function. *J Biol Chem* 2011; **286**: 15980–15988.
42 Arora D, Stopp S, Bohmer SA, Schons J, Godfrey R, Masson K *et al.* Protein-tyrosine phosphatase DEP-1 controls receptor tyrosine kinase FLT3 signaling. *J Biol Chem* 2011; **286**: 10918–10929.
43 Flint AJ, Tiganis T, Barford D, Tonks NK. Development of 'substrate-trapping' mutants to identify physiological substrates of protein tyrosine phosphatases. *Proc Natl Acad Sci USA* 1997; **94**: 1680–1685.
44 Chu P, Clanton DJ, Snipas TS, Lee J, Mitchell E, Nguyen ML *et al.* Characterization of a subpopulation of colon cancer cells with stem cell-like properties. *Int J Cancer J Int Cancer* 2009; **124**: 1312–1321.
45 Wang J, Sakariassen PO, Tsinkalovsky O, Immervoll H, Boe SO, Svendsen A *et al.* CD133 negative glioma cells form tumors in nude rats and give rise to CD133 positive cells. *Int J Cancer J Int Cancer* 2008; **122**: 761–768.
46 Shmelkov SV, Butler JM, Hooper AT, Hormigo A, Kushner J, Milde T *et al.* CD133 expression is not restricted to stem cells, and both CD133+ and CD133− metastatic colon cancer cells initiate tumors. *J Clin Invest* 2008; **118**: 2111–2120.
47 Wei Y, Jiang Y, Zou F, Liu Y, Wang S, Xu N *et al.* Activation of PI3K/Akt pathway by CD133–p85 interaction promotes tumorigenic capacity of glioma stem cells. *Proc Natl Acad Sci USA* 2013; **110**: 6829–6834.
48 Lombardo Y, Scopelliti A, Cammareri P, Todaro M, Iovino F, Ricci-Vitiani L *et al.* Bone morphogenetic protein 4 induces differentiation of colorectal cancer stem cells and increases their response to chemotherapy in mice. *Gastroenterology* 2011; **140**: 297–309.
49 Ricci-Vitiani L, Mollinari C, di Martino S, Biffoni M, Pilozzi E, Pagliuca A *et al.* Thymosin beta4 targeting impairs tumorigenic activity of colon cancer stem cells. *FASEB J* 2010; **24**: 4291–4301.
50 Talamonti MS, Roh MS, Curley SA, Gallick GE. Increase in activity and level of pp60c-src in progressive stages of human colorectal cancer. *J Clin Invest* 1993; **91**: 53–60.
51 Aligayer H, Boyd DD, Heiss MM, Abdalla EK, Curley SA, Gallick GE. Activation of Src kinase in primary colorectal carcinoma: an indicator of poor clinical prognosis. *Cancer* 2002; **94**: 344–351.
52 Chen YS, Wu MJ, Huang CY, Lin SC, Chuang TH, Yu CC *et al.* CD133/Src axis mediates tumor initiating property and epithelial-mesenchymal transition of head and neck cancer. *PLoS ONE* 2011; **6**: e28053.
53 Bläker H, Mechtersheimer G, Sutter C, Hertkorn C, Kern MA, Rieker RJ *et al.* Recurrent deletions at 6q in early age of onset non-HNPCC- and non-FAP-associated intestinal carcinomas. Evidence for a novel cancer susceptibility locus at 6q14–q22. *Genes Chromosomes Cancer* 2008; **47**: 159–164.
54 Starr TK, Allaei R, Silverstein KAT, Staggs RA, Sarver AL, Bergemann TL *et al.* A transposon-based genetic screen in mice identifies genes altered in colorectal cancer. *Science* 2009; **323**: 1747–1750.
55 Novellino L, De Filippo A, Deho P, Perrone F, Pilotti S, Parmiani G *et al.* PTPRK negatively regulates transcriptional activity of wild type and mutated oncogenic beta-catenin and affects membrane distribution of beta-catenin/E-cadherin complexes in cancer cells. *Cell Signal* 2008; **20**: 872–883.
56 Mak AB, Nixon AM, Kittanakom S, Stewart JM, Chen GI, Curak J *et al.* Regulation of CD133 by HDAC6 promotes beta-catenin signaling to suppress cancer cell differentiation. *Cell Rep* 2012; **2**: 951–963.
57 Ochiai H, Takenobu H, Nakagawa A, Yamaguchi Y, Kimura M, Ohira M *et al.* Bmi1 is a MYCN target gene that regulates tumorigenesis through repression of KIF1B-beta and TSLC1 in neuroblastoma. *Oncogene* 2010; **29**: 2681–2690.
58 Kurata K, Yanagisawa R, Ohira M, Kitagawa M, Nakagawara A, Kamijo T. Stress via p53 pathway causes apoptosis by mitochondrial Noxa upregulation in doxorubicin-treated neuroblastoma cells. *Oncogene* 2007; **27**: 741–754.
59 Komatsu S, Takenobu H, Ozaki T, Ando K, Koida N, Suenaga Y *et al.* Plk1 regulates liver tumor cell death by phosphorylation of TAp63. *Oncogene* 2009; **28**: 3631–3641.
60 Kubo N, Wu D, Yoshihara Y, Sang M, Nakagawara A, Ozaki T. Co-chaperon DnaJC7/TPR2 enhances p53 stability and activity through blocking the complex formation between p53 and MDM2. *Biochem Biophys Res Commun* 2013; **430**: 1034–1039.
61 Kondo J, Endo H, Okuyama H, Ishikawa O, Iishi H, Tsujii M *et al.* Retaining cell–cell contact enables preparation and culture of spheroids composed of pure primary cancer cells from colorectal cancer. *Proc Natl Acad Sci USA* 2011; **108**: 6235–6240.

Supplementary Information accompanies this paper on the Oncogene website (http://www.nature.com/onc)

VOLUME 32 · NUMBER 28 · OCTOBER 1 2014

JOURNAL OF CLINICAL ONCOLOGY

ORIGINAL REPORT

Kieuhoa T. Vo, Katherine K. Matthay, John Neuhaus, and Steven G. DuBois, Benioff Children's Hospital and University of California, San Francisco, San Francisco; Doug Miniati, Kaiser Permanente Medical Center, Roseville, CA; Wendy B. London, Children's Oncology Group Statistics and Data Center and Dana-Farber Children's Hospital Cancer Center, Boston, MA; Barbara Hero, Children's Hospital, University of Cologne, Köln, Germany; Peter F. Ambros, Children's Cancer Research Institute, St Anne Kinderkrebsforschung, Vienna, Austria; Akira Nakagawara, Chiba Cancer Center Research Institute and Chiba University, Chiba, Japan; Kate Wheeler, Oxford Children's Hospital, Oxford; Andrew D.J. Pearson, Institute of Cancer Research and Royal Marsden Hospital, Surrey, United Kingdom; Susan L. Cohn, The University of Chicago, Chicago, IL.

Published online ahead of print at www.jco.org on August 25, 2014.

Support information appears at the end of this article.

Terms in blue are defined in the glossary, found at the end of this article and online at www.jco.org.

Data included in the International Neuroblastoma Risk Group database were provided by the Children's Oncology Group (COG), Pediatric Oncology Group (POG), Children's Cancer Study Group (CCSG), German Gesellschaft für Pädiatrische Onkologie und Hämatologie (GPOH), European Neuroblastoma Study Group (ENSG), International Society of Paediatric Oncology Europe Neuroblastoma Group (SIOPEN), Japanese Advanced Neuroblastoma Study Group (JANB), Japanese Infantile Neuroblastoma Co-operative Study Group (JINCS), Spanish Neuroblastoma Group, and Italian Neuroblastoma Group. The contents are solely the responsibility of the authors and do not necessarily represent the official views of the funding sources listed.

Authors' disclosures of potential conflicts of interest and author contributions are found at the end of this article.

Corresponding author: Steven G. DuBois, MD, Department of Pediatrics, University of California, San Francisco School of Medicine, Benioff Children's Hospital, 505 Parnassus Ave, M646, San Francisco, CA 94143-0106; e-mail: duboiss@peds.ucsf.edu.

0732-183X/14/3228w-3169w/$20.00

DOI: 10.1200/JCO.2014.56.1621

Clinical, Biologic, and Prognostic Differences on the Basis of Primary Tumor Site in Neuroblastoma: A Report From the International Neuroblastoma Risk Group Project

Kieuhoa T. Vo, Katherine K. Matthay, John Neuhaus, Wendy B. London, Barbara Hero, Peter F. Ambros, Akira Nakagawara, Doug Miniati, Kate Wheeler, Andrew D.J. Pearson, Susan L. Cohn, and Steven G. DuBois

ABSTRACT

Purpose
Neuroblastoma (NB) is a heterogeneous tumor arising from sympathetic tissues. The impact of primary tumor site in influencing the heterogeneity of NB remains unclear.

Patients and Methods
Children younger than age 21 years diagnosed with NB or ganglioneuroblastoma between 1990 and 2002 and with known primary site were identified from the International Neuroblastoma Risk Group database. Data were compared between sites with respect to clinical and biologic features, as well as event-free survival (EFS) and overall survival (OS).

Results
Among 8,369 children, 47% had adrenal tumors. All evaluated clinical and biologic variables differed statistically between primary sites. The features that were > 10% discrepant between sites were stage 4 disease, *MYCN* amplification, elevated ferritin, elevated lactate dehydrogenase, and segmental chromosomal aberrations, all of which were more frequent in adrenal versus nonadrenal tumors ($P < .001$). Adrenal tumors were more likely than nonadrenal tumors (adjusted odds ratio, 2.09; 95% CI, 1.67 to 2.63; $P < .001$) and thoracic tumors were less likely than nonthoracic tumors (adjusted odds ratio, 0.20; 95% CI, 0.11 to 0.39; $P < .001$) to have *MYCN* amplification after controlling for age, stage, and histologic grade. EFS and OS differed significantly according to the primary site ($P < .001$ for both comparisons). After controlling for age, *MYCN* status, and stage, patients with adrenal tumors had higher risk for events (hazard ratio, 1.13 compared with nonadrenal tumors; 95% CI, 1.03 to 1.23; $P = .008$), and patients with thoracic tumors had lower risk for events (HR, 0.79 compared with nonthoracic; 95% CI, 0.67 to 0.92; $P = .003$).

Conclusion
Clinical and biologic features show important differences by NB primary site, with adrenal and thoracic sites associated with inferior and superior survival, respectively. Future studies will need to investigate the biologic origin of these differences.

J Clin Oncol 32:3169-3176. © 2014 by American Society of Clinical Oncology

INTRODUCTION

One of the hallmarks of neuroblastoma (NB) is its clinical and biologic heterogeneity. The likelihood of cure is dependent on widely varying factors, including age, disease stage, tumor site, and biologic features.[1-3] The impact of the primary site of disease in influencing the heterogeneity of NB remains unclear.

Previous work has suggested that extra-abdominal NB tumors (cervical, thoracic, pelvic) may be associated with more favorable clinical and biologic characteristics and therefore a better outcome compared with NBs that originate from the abdomen.[4] In a retrospective analysis of 143 patients with NB, the frequency of stage 4 disease, tumor *MYCN* gene amplification, elevated lactate dehydrogenase (LDH), and elevated ferritin were all significantly lower in the extra-abdominal group than in the abdominal group. Not surprisingly, the probability of 5-year event-free survival (EFS) was higher in the extra-abdominal group (94%) than in the abdominal group (69%); however, a multivariable analysis was not performed in this study.[4] Studies focused on pelvic NB have shown conflicting results. One study observed that pelvic primary tumor sites were mainly associated with advanced disease.[5] Other studies reported that pelvic tumors represent a more favorable prognostic subgroup, particularly among patients with higher-stage disease.[6,7]